

Geology of the
East-Central San Mateo Mountains,
Socorro County, New Mexico

by

Charles A. Ferguson

Submitted in partial fulfillment
of the Requirements for the Degree of
Master of Science in Geology

New Mexico Institute of Mining and Technology,

Socorro, New Mexico

September, 1985

ABSTRACT

The San Mateo Mountains, composed dominately of felsic volcanic and volcanoclastic rocks, are a north-trending Basin and Range uplift on the northeast corner of the mid-Tertiary Datil-Mogollon volcanic field in Socorro County, New Mexico. Detailed mapping shows that the four youngest of the five Oligocene regional rhyolite ash-flow tuffs in the Socorro area (oldest to youngest: La Jencia; Vicks Peak; Lemitar; and South Canyon Tuffs) are exposed in the east-central part of the range.

In the southern part of the study area, the Vicks Peak Tuff thickens (100m to >300m) from east to west where it is eventually buried by local volcanic units. This, together with similar relationships farther south, suggest that a syn-volcanic depression of Vicks Peak age is located in the south-central part of the San Mateo Mountains. Subsequent resurgence of this area is indicated by southwestward thinning of the next youngest unit (Lemitar Tuff).

A northeast trending west-side down fault zone, which truncates rocks older than the South Canyon Tuff, forms a structural basin in the western half of the study area. Stratigraphic relations along this fault zone show that it was activated during the eruption of the South Canyon Tuff. The structural basin to the northwest of this fault zone is filled with >600m of the South Canyon Tuff, and is thought

to be the south end of it's cauldron. The structural basin continues into the southwest corner of the study area where it is filled with about 200m of pre-South Canyon volcanoclastic rocks (west-fining alluvial fan complex) and rhyolite lava. Eolian sandstones in this sequence were deposited by prevailing southwest winds.

All igneous rocks indigenous to this study area are high-SiO₂ (>75%), high-K₂O (5%) rhyolites. Paleomagnetically, all of the ash-flow tuffs in the study area are reversely polarized, except for the Lemitar Tuff.

Basin and Range faulting, the result of a late Oligocene least principle stress field oriented about N63E, was initiated during the waning stages of ash-flow tuff volcanism in the study area. The Oligocene strata dips east from 5 to 50 degrees, with the amount of extension (proportional to tilting) increasing from 20% to 100% from south to north in the study area. North-south trending west-side down faults are found throughout the study area, but east-west south-side down faults are found only in the southern part. This change in structural style occurs across the proposed South Canyon Tuff cauldron margin, and was probably controlled by a shallow (3km) pluton beneath this cauldron in the north, and pre-Tertiary basement structures in the south.

TABLE OF CONTENTS

CHAPTER 1 INTRODUCTION.....	1
Location.....	1
Previous work.....	3
Purpose.....	6
Procedures.....	6
Acknowledgements.....	7
 CHAPTER 2 UNIT DESCRIPTIONS.....	 9
Introduction.....	9
Basaltic Andesite.....	9
La Jencia Tuff.....	11
Distribution.....	11
Petrography.....	12
Vicks Peak Tuff.....	14
Distribution.....	14
Petrography.....	18
Tuff of The Park.....	23
Distribution.....	23
Petrography.....	25
First stage rhyolites.....	27
Rhyolite of Drift Fence Canyon.....	27
Distribution.....	27
Petrography.....	31
Rhyolite of Exter Canyon.....	31
Distribution.....	31
Petrography.....	31
Lemitar Tuff.....	32
Distribution.....	32
Petrography.....	33
Second stage rhyolites.....	36
Distribution.....	36
Petrography.....	37
Unit of East Red Canyon.....	38
Distribution.....	38
Petrography.....	40
Stratigraphic sections.....	52
Paleontology.....	56
South Canyon Tuff.....	59
Distribution.....	59
Members of the South Canyon Tuff.....	49
Petrography.....	61
Hydrothermal alteration.....	69
Units younger than the South Canyon Tuff.....	70
Unit of North Canyon.....	70
Intrusive Rhyolite of Wildcat Peak.....	71
Tuff of Rosedale Canyon.....	72

CHAPTER 3 STRATIGRAPHY.....	73
Introduction.....	73
Correlation with previous work.....	75
Stratigraphy in this area.....	79
Introduction.....	79
Units older than Lemitar Tuff.....	79
La Jencia Tuff.....	79
Vicks Peak Tuff.....	80
Tuff of The Park.....	80
Lemitar Tuff.....	81
Unit of East Red Canyon.....	81
South Canyon Tuff.....	82
Intrusive Rhyolites.....	83
Summary.....	84
 CHAPTER 4 STRUCTURE.....	 86
Introduction.....	86
Volcanic structures.....	86
Structures related to the Vicks Peak Tuff.....	86
Structures related to the South Canyon Tuff.....	88
South Canyon Tuff cauldron margin.....	88
Sedimentary basin of the unit of East Red Canyon..	91
Basin and Range structures.....	93
Fault patterns and the least principle stress field..	93
Magnitude of tilting and the age of Basin and Range extension.....	96
Summary.....	97
 CHAPTER 5 CHEMISTRY.....	 99
Introduction.....	99
Ash-flow tuffs.....	102
Intrusives.....	102
 CHAPTER 6 PALEOMAGNETISM.....	 104
Introduction.....	104
Polarity.....	105
Anisotropy of Susceptibility.....	105
 CHAPTER 7 CONCLUSIONS.....	 108
 POSTSCRIPT.....	 110
 REFERENCES.....	 112
 APPENDIX A PETROGRAPHIC PROCEDURES.....	 115
 APPENDIX B GEOCHEMICAL PROCEDURES.....	 116
 APPENDIX C PALEOMAGNETIC PROCEDURES.....	 117

LIST OF FIGURES

Figure 1. Topographic map of Socorro County showing the study area (stippled), and proposed cauldrons in the San Mateo Mountains.....	2
Figure 2. Location map of the study area showing forest roads, major drainages, and political boundaries....	4
Figure 3. Photograph of basaltic andesite lava.....	10
Figure 4. Stratigraphic section of the La Jencia Tuff.....	13
Figure 5. Outcrop map of the La Jencia Tuff.....	15
Figure 6. Photographs of lineated pumice in the Vicks Peak Tuff.....	20
Figure 7. Outcrop map of the Vicks Peak Tuff.....	21
Figure 8. Stratigraphic section of the Vicks Peak Tuff....	22
Figure 9. Outcrop map of the tuff of The Park and the Lemitar Tuff.....	24
Figure 10. Stratigraphic section of the tuff of The Park..	26
Figure 11. Outcrop map of the rhyolite lava of Drift Fence Canyon.....	29
Figure 12. Outcrop map of the Lemitar Tuff showing the distribution of paleocanyon walls buried by the unit.....	30
Figure 13. Stratigraphic section of the Lemitar Tuff.....	35
Figure 14. Outcrop map of the unit of East Red Canyon.....	39
Figure 15(a). Generalized stratigraphic sections of the unit of East Red Canyon.....	41
Figure 15(b). Detailed stratigraphic section of eolian sandstone in the unit of East Red Canyon.....	42
Figure 16. Photograph of matrix supported diamictite.....	44
Figure 17. Photograph of basal portion of a cross-stratified sandstone set.....	46
Figure 18. Photograph of cliff of eolian sandstone.....	48
Figure 19. Block diagram showing a possible origin of the first order bounding surfaces observed in the unit of East Red Canyon.....	49

Figure 20. Photograph of bedded ash-flow tuff.....	50
Figure 21. Photograph of desiccation cracks in a mudstone bed.....	51
Figure 22. Rose diagram of paleocurrent directions from eolian sandstone in the unit of East Red Canyon.....	55
Figure 23. Photograph of arctiodactyl hoof print molds in a slab of bedded tuff.....	57
Figure 24. Photograph of inclined burrow.....	58
Figure 25. Outcrop map of the South Canyon Tuff.....	62
Figure 26. Stratigraphic section of the South Canyon Tuff.....	64
Figure 27. Photograph of lineated pumice in the South Canyon Tuff.....	67
Figure 28. Outcrop map of the South Canyon Tuff.....	68
Figure 29. Stratigraphic sequence from this study compared with the regional stratigraphy of Osburn and Chapin (1983).....	74
Figure 30. Stratigraphic sequence from this study compared with the stratigraphic sequences of previous workers in adjacent areas.....	76
Figure 31. Structural map of the study area showing the extent of structural depressions filled by the Vicks Peak Tuff, the unit of East Red Canyon, and the South Canyon Tuff.....	87
Figure 32. Four stage model for the formation of the southeast structural margin of the South Canyon Tuff's cauldron.....	90
Figure 33. Structural map of the study area showing the moderately extended domain, and the weakly extended domain.....	94
Figure 34. Paleomagnetic pole positions for samples of the La Jencia Tuff, Vicks Peak Tuff, tuff of The Park, and the Lemitar Tuff.....	106
Figure 35. Paleomagnetic pole positions for samples of the South Canyon Tuff, and the tuff of Rosedale Canyon..	107

LIST OF PLATES AND TABLES

Plate 1. Geologic Map.....(in pocket)

Plate 2. East-West Cross Sections.....(in pocket)

Plate 3. North-South Cross Sections.....(in pocket)

Plate 4. Sample Location Map.....(in pocket)

Table 1. Percentages of grain types in eolian sandstones from the unit of East Red Canyon.....54

Table 2. Petrographic data from samples of the South Canyon Tuff (not including data from Figure 26.) throughout the study area.....65

Table 3. The location and age constraints of dikes in the study area whose trends are thought to have been determined by a regional stress field.....95

Table 4. Major element chemical data of the South Canyon Tuff, Lemitar Tuff, and the tuff of The Park....100

Table 5. Major element chemical data of rhyolite intrusives in the study area.....101

CHAPTER 1

INTRODUCTION

Location

The San Mateo Mountains are a north-trending (40 by 15 mile) Basin and Range uplift in the southwest corner of Socorro County, New Mexico. They are composed predominately of Oligocene silicic ash-flow tuffs, lavas, and related volcanoclastic rocks. Paleozoic sedimentary and Precambrian crystalline rocks are exposed in the extreme southeast corner of the range. Elevations increase from less than 6,000 feet in the southern foot hills to well over 10,000 feet in the north and south ends of the range (Fig. 1). The elevated region to the north has been interpreted as the resurgent dome of the Mt. Withington Caldera (Deal, 1973, Deal and Rhodes, 1976). The elevated region to the south is mostly unmapped, but the proposed Nogal Canyon Caldera (Deal and Rhodes, 1976) overlaps the southeast part of it. The study area, with which this project is concerned, is a 50 square mile block centered on the eastern half of a prominent saddle that separates these higher areas (Fig. 1).

Total topographic relief in the study area is just under 4,000 feet. Vegetation below 7,000 feet consists of high prairie grasses, with rare juniper and white oak in

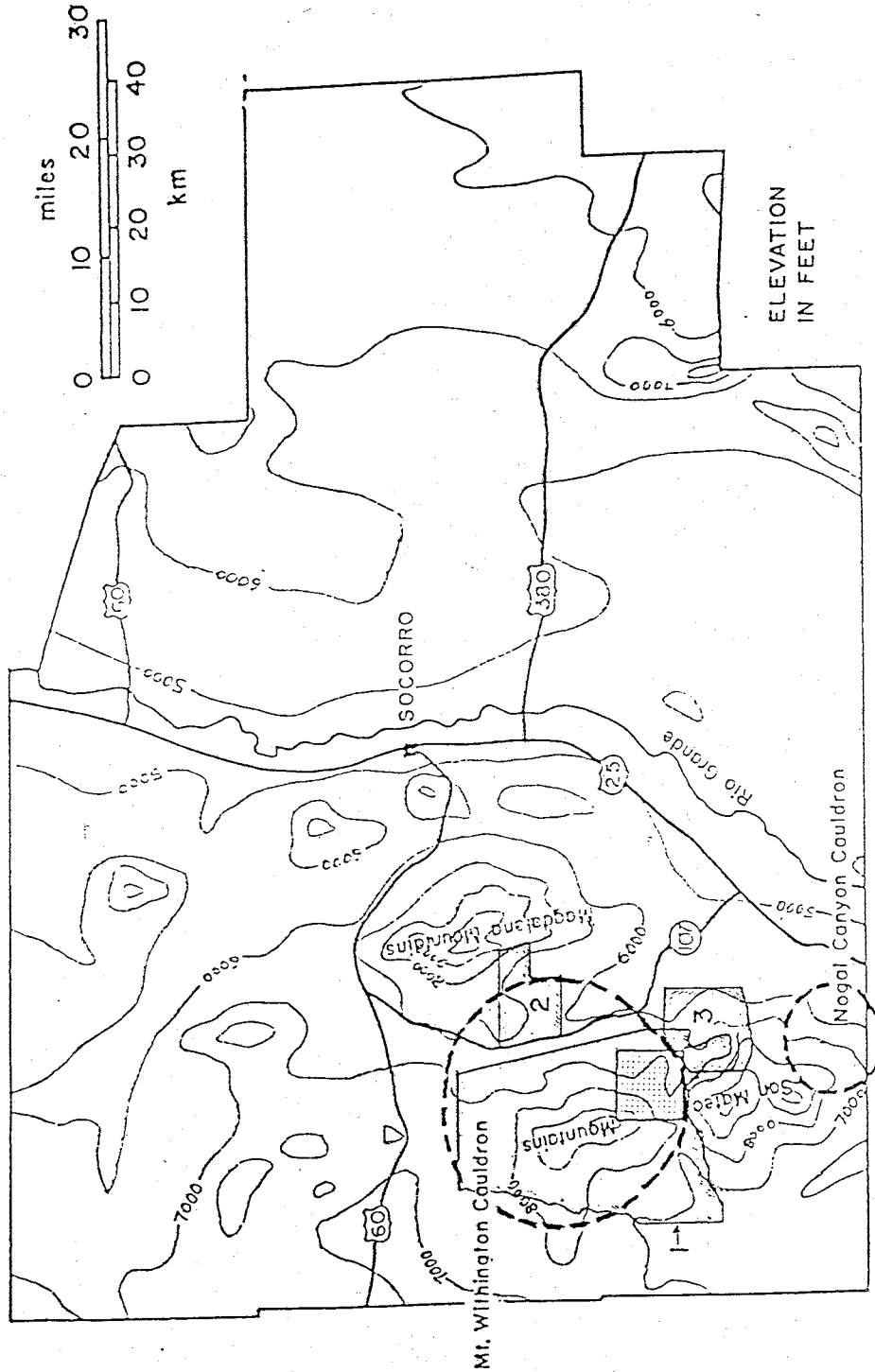


Figure 1. Topographic map of Socorro County showing the study area (stippled), proposed cauldrons in the San Mateo Mountains, and map areas of adjacent workers: 1) Deal (1973); 2) Donze (1980); and 3) Atwood (1982).

sheltered arroyos and canyons. Mixed juniper, pinon pine, oak, and ponderosa pine occupy elevations from 7,000 to 8,000 feet. Above 8,000 feet ponderosa pine is mixed with douglas fir and spruce, and on north-facing slopes groves of aspen are common. No correlation between vegetation and rock type was observed in the study area.

All of the study area is located within Cibola National Forest, except for six sections in the northeast corner. Major access roads include three forest roads (Fig. 2), and in the northeast corner a system of private ranch roads. The forest roads can be negotiated with high clearance two wheel drive vehicles. Travel on the ranch roads requires four-wheel drive, and permission from local ranchers.

The study area is deeply dissected by three major east-flowing drainages; Rosedale Canyon, North Canyon, and East Red Canyon (Fig. 2). These canyons usually contain no running water, but host several springs with drinkable water in the western part of the study area. All major springs are located on the upslope (west) side of north-trending normal faults.

Previous work

Reconnaissance mapping of the northern San Mateo Mountains by Deal (1973) revealed great thicknesses of two major ash-flow tuff units (A-L Peak Tuff, and the Potato

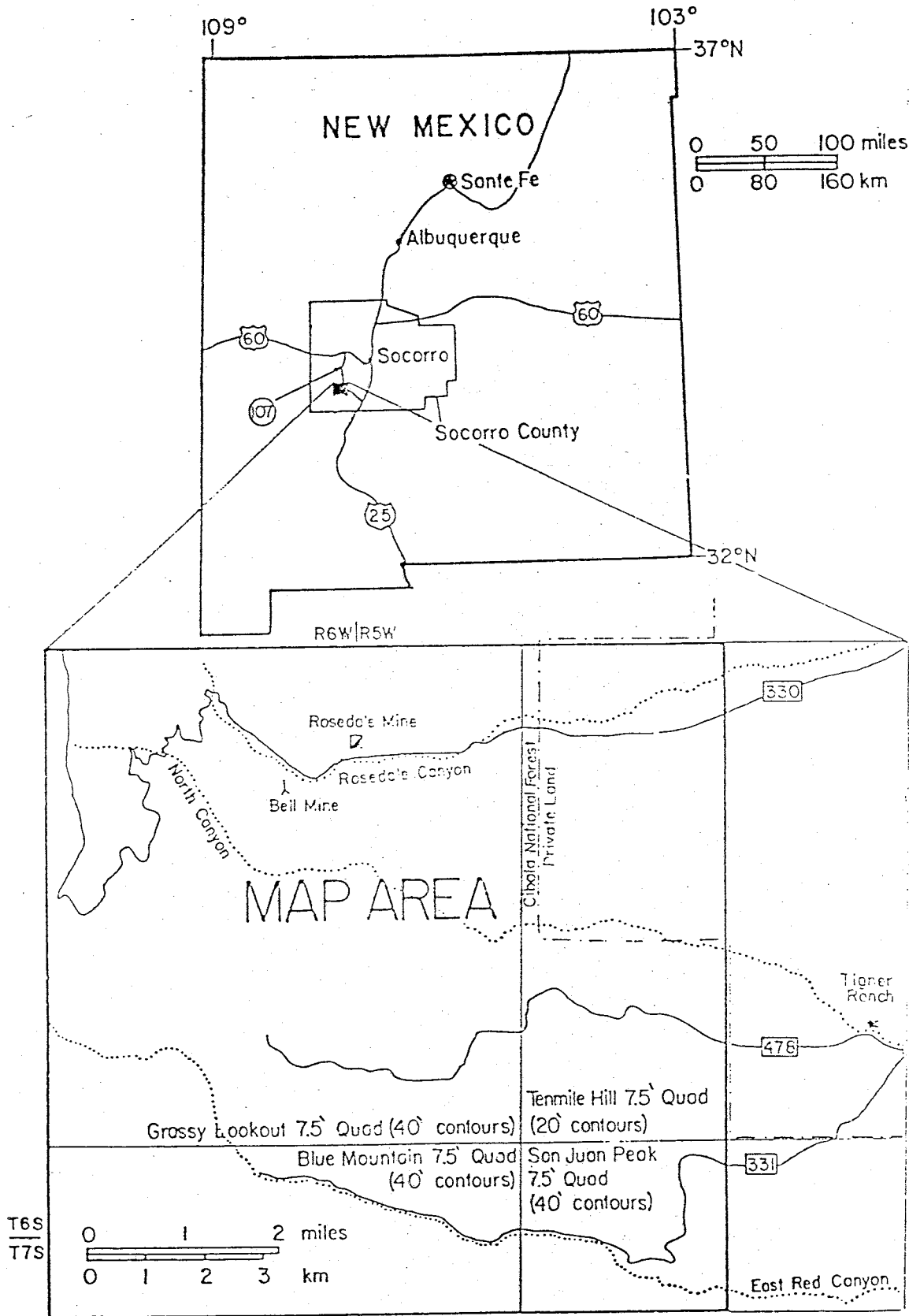


Figure 2. Location map of the study area showing forest roads, major drainages, and political boundaries.

Canyon Tuff). Deal (1973) proposed the Mt. Withington cauldron as the source for these two tuffs. In the central part of the range, Deal mapped a sequence of volcanoclastic sediments, rhyolite lavas, and tuffs overlying the cauldron-filling tuffs. These rocks were grouped into the Beartrap Canyon Formation which was interpreted as a moat sequence for the Mt. Withington cauldron.

Donze (1980) mapped an area about 6km northeast of this study area in a range of hills connecting the Magdalena Range with the north end of the San Mateos (Fig. 1). His map shows at least 670m of Lemitar Tuff with no exposed base. This Lemitar Tuff correlates with the cauldron-filling Potato Canyon Tuff of Deal (1973), and is overlain by 60-300m of volcanoclastic sediment and 50-100m of South Canyon Tuff. Osburn and Chapin (1983) have shown that the Lemitar Tuff, as mapped by Donze (1980), is actually the South Canyon Tuff, and his South Canyon Tuff is a local intracaldera tuff (see discussion in Chapter 3).

Mapping by Atwood (1982) in an area adjacent to the southeast corner of this study area revealed great thicknesses of Vicks Peak Tuff (400m). The Vicks Peak Tuff is thought to originate from the Nogal Canyon cauldron (Fig. 1) which is older than the Mt. Withington cauldron. Atwood's map shows the Vicks Peak Tuff truncated to the southwest (directly south of this study area) by a major

west-side down fault. Across this fault, Vicks Peak Tuff is buried by about 300m of ash-flow tuff, volcanoclastic sediment, and rhyolite lava that was correlated with the Beartrap Canyon Formation of Deal (1973).

Purpose

The purpose of this study is four fold: (1) define stratigraphy for the central San Mateo Mountains and to correlate it with stratigraphy already established to the northeast (Osburn and Chapin, 1983); (2) investigate the margin of the proposed Mt. Withington cauldron, and a possible older volcanic structure related to the Vicks Peak Tuff to the southwest; (3) examine lateral changes in style of basin and range deformation within the study area; and (4) geochemically characterize the major volcanic units.

Procedures

Detailed geologic mapping was done by the author in the summer-fall of 1983, and the spring of 1984 using 1:24,000 scale, U.S.G.S., 7.5 minute, topographic quadrangles (Fig. 2), supplemented by 1:50,000 scale, 1935 Soil Conservation Survey, aerial photographs 8468-8473, 8486-8490, and 8514-8518. All information on the geologic map (Plate 1) and cross sections (Plate 2,3) was compiled by the author solely from his field maps and notes.

All petrographic and geochemical samples were collected between the summers of 1983 and 1984. Oriented core samples for paleomagnetic studies of principle units were collected in the spring of 1984, and spring 1985 by Bill McIntosh and the author. Plate 4 is a location map for all petrographic, geochemical, and paleomagnetic samples for which observations and or data are presented in this paper. The author is responsible for all petrographic observations, and for the preparation of samples for major-element geochemical analyses (X-ray fluorescence) except for samples (84-27,159) which were done by G. R. Osburn of the New Mexico Bureau of Mines and Mineral Resources.

Petrographic, geochemical, and paleomagnetic procedures are described in Appendices A, B, and C, respectively.

Acknowledgments

I would like to thank the New Mexico Bureau of Mines and Mineral Resources for providing field support vehicles, and for funding geochemical analyses, and thin section costs. I would also like to thank Bob Osburn, Bill McIntosh, and Dave Johnson for helpful comments in the field, and Ken Lemley for processing my sedimentary paleocurrent data. Bob Osburn, Dave Johnson, and Phil Kyle critically reviewed the manuscript, and served on the thesis committee. Fletcher and Lucille Tigner allowed access to

their private land, assisted with mechanical problems, and located unmapped springs that saved me a great deal of time and trouble.

CHAPTER 2
UNIT DESCRIPTIONS

Introduction

In this chapter, detailed descriptions of each map unit are presented in ascending stratigraphic order. The description of each unit will include the following observations: (1) stratigraphic position; (2) thickness, and lateral variations in thickness; (3) description of upper and lower contacts; (4) hand specimen and/or field descriptions of macroscopic textures; and (5) micropetrographic descriptions of selected units.

Basaltic Andesite (unnamed)

The oldest unit exposed in the study area is a basaltic andesite lava flow, which crops out sporadically over an area of about one square mile in the east-central part. The lateral extent of the flow is unknown, and since its lower contact is not exposed only a minimum thickness, of 60 meters, could be determined.

The best exposure of the lava is in North Canyon where it is nonvesicular and brecciated, and is interpreted as a blocky flow (Fig. 3). South of here, the lava is usually vesicular and non-brecciated. Based on field and hand

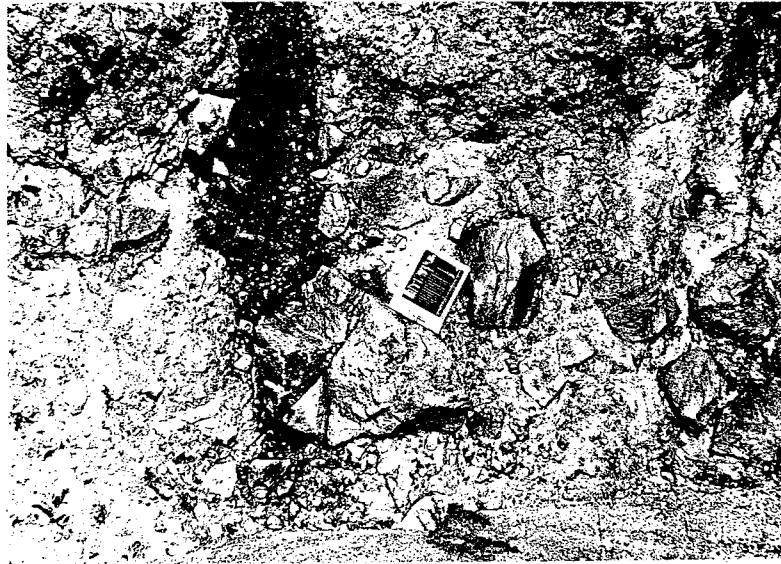


Figure 3. Photograph of brecciated basaltic andesite lava (sec. 15, T6S, R5W), which is interpreted to be a blocky flow.

sample examination, the lava contains about 5% plagioclase (1-2mm) and about 3% ferromagnesian phenocrysts (1mm). The ferromagnesian minerals could not be identified, because they were oxidized. The groundmass is grayish-red-purple in color, and can be massive or vesicular.

La Jencia Tuff

Distribution

The La Jencia Tuff (Osburn and Chapin, 1983) is a crystal-poor rhyolite ash-flow tuff, whose source is the composite Sawmill Canyon-Magdalena Cauldron in the central Magdalena Mountains. The La Jencia Tuff, formerly the A-L Peak Tuff (Deal, 1973; Deal and Rhodes, 1976), is the oldest regional unit in the study area. It was originally described by Tonking (1957) as the middle part of the Hells Mesa member of the Datil Formation, and by Brown (1972) as the lower tuff of Bear Springs. Deal (1973) miscorrelated this unit with a younger tuff on A-L Peak (northern San Mateo Mountains) which was actually the South Canyon Tuff (Osburn and Chapin, 1983).

The La Jencia Tuff is exposed only in the southeast part of the study area, and is conformably overlain by The Vicks Peak Tuff, in most places. In North Canyon, paleocanyons filled with Lemitar Tuff cut through the Vicks

Peak Tuff into its upper part. The unit's base, exposed only in the North Canyon area, consists of a poorly-welded interval (<3m) which rests on basaltic andesite lava. In North Canyon the unit is divided into a lower massive member (70m) and an upper flow-banded member, whose top is not exposed. In East Red Canyon the massive member is not exposed, but about 200m of the flow-banded member is, making the unit at least 270m thick. Along the walls of East Red Canyon, the flow banded member weathers into distinct ledges separated by 5-15m high cliffs which may represent individual flow-units.

Petrography

Three thin sections of the La Jencia Tuff were studied (83-78, 83-133, 84-19; Fig. 4). Phenocrysts throughout the unit are mostly euhedral blocky or tabular sanidine (2-3mm), with minor amounts of subhedral quartz (1mm), and trace amounts of biotite (0.5mm), sphene (0.5mm), plagioclase (0.2mm), and opaque minerals (0.2mm). Above the unwelded base, the massive member is a pale-red densely welded tuff containing about 7% phenocrysts. It contains about 5% pumice that average 1-3cm in length, and have compaction ratios of about 12:1. The transition from massive to flow-banded members occurs over a 20m interval defined by a rapid increase in pumice content (5-25%), and a slight decrease in phenocryst content (7-5%).

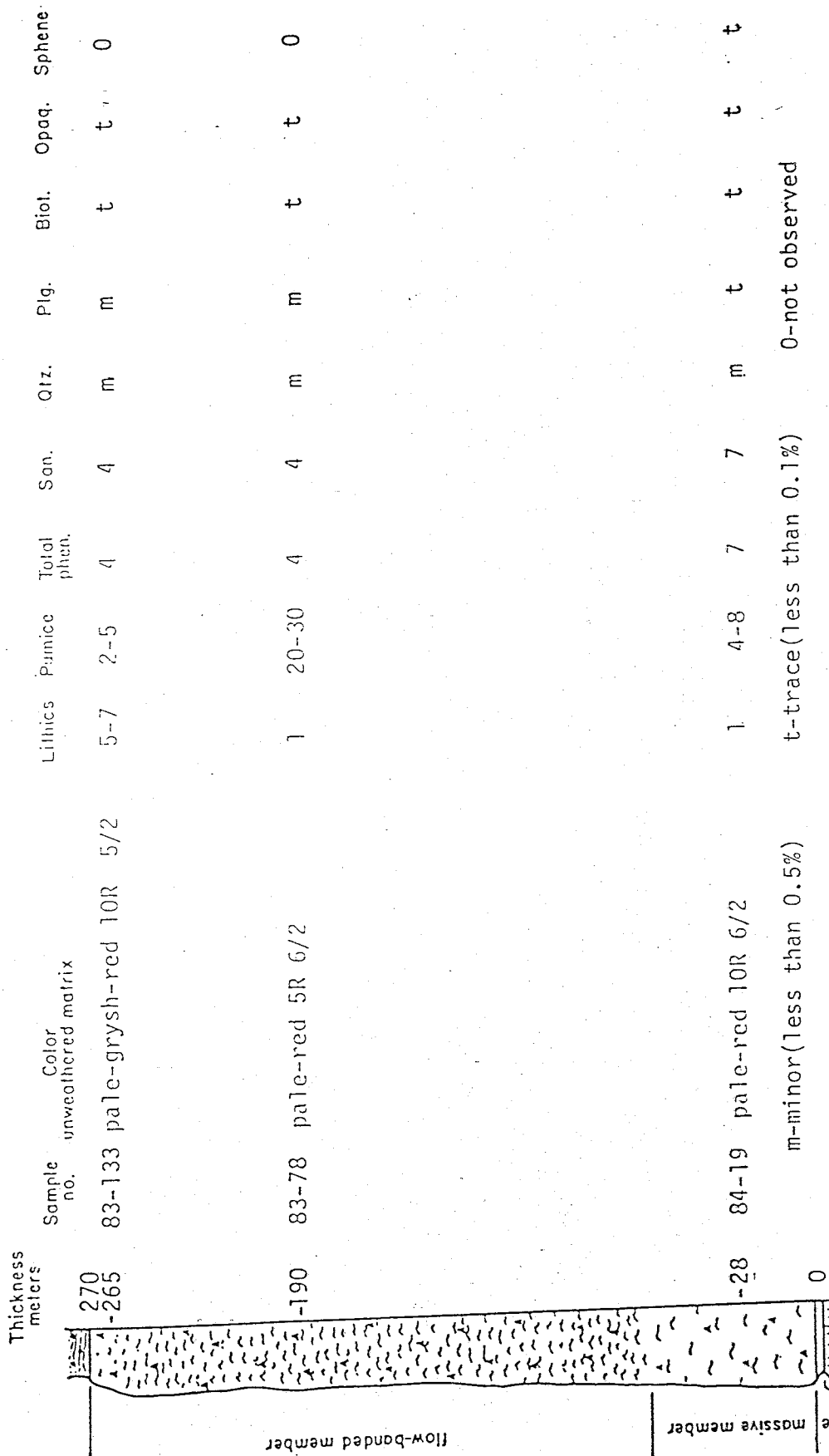


Figure 4. Stratigraphic section of the La Jencia Tuff (sec. 15, T6S, R5W, and sec. 32, T6S, R5W). Visual estimates of phenocryst percentages are from thin sections, and lithic and pumice percentages are estimated from hand specimens.

--- Pumice fragments.
 .. Lithic fragments
 ▲ Phenocrysts

The flow-banded member, also pale-red and densely welded, is characterized by exceptionally flattened and elongated pumice fragments (compaction ratios $>50:1$). The extreme elongation of pumice fragments (up to 0.5m) defines a pronounced east-west lineation that is consistent throughout the study area (Fig. 5). The azimuth to the source of the La Jencia Tuff (central Magdalena Mountains) is almost perpendicular to flow-lineation azimuths measured in this study. This probably reflects the effect of regional slope on the orientation of flow indicators in the unit.

The top of the La Jencia Tuff, where it is preserved, is grayish-red and moderately welded. Small ($<3\text{cm}$) uncompact pumice compose only about 4% of this tuff, but its phenocryst assemblage is similar to the rest of the unit.

Vicks Peak Tuff

Distribution

The Vicks Peak Tuff (Furlow, 1965; Deal and Rhodes, 1976) is a densely welded crystal-poor rhyolite ash-flow tuff similar to the underlying La Jencia Tuff. The source of the Vicks Peak Tuff is thought to be in the southeast San Mateo Mountains (Nogal Canyon cauldron) where Deal and Rhodes

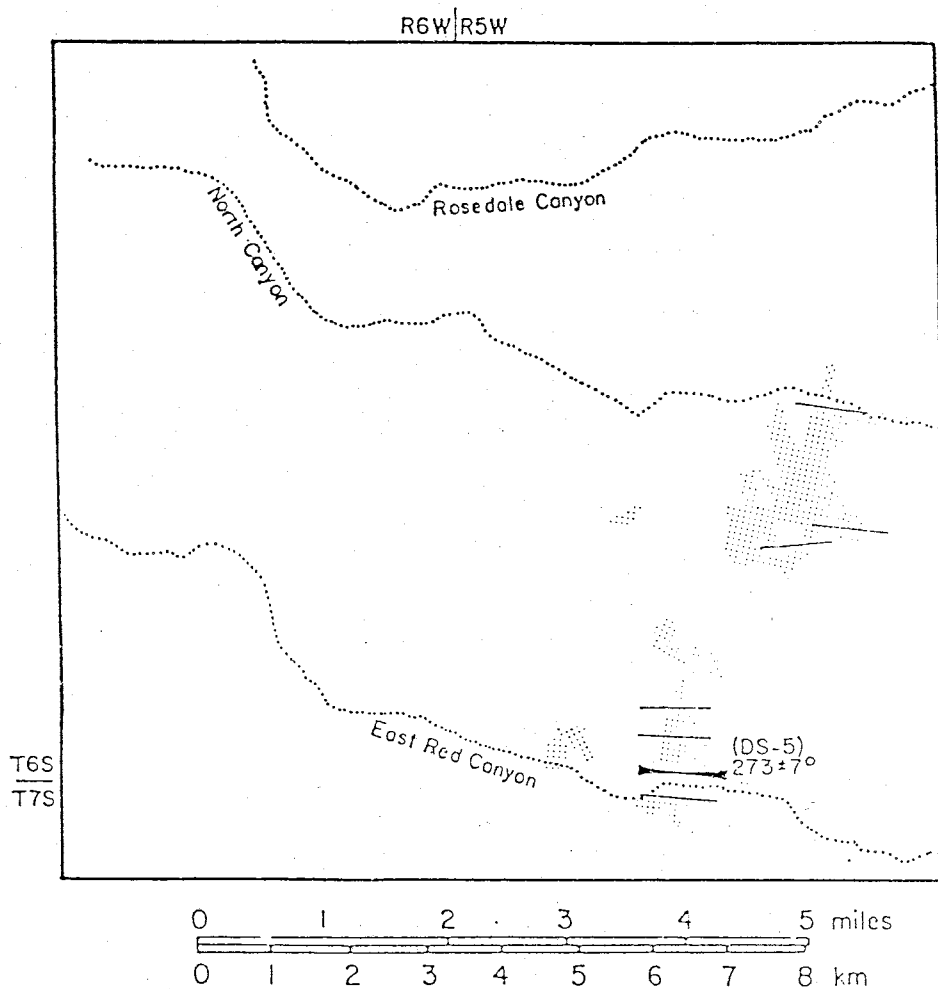


Figure 5. Outcrop map of the La Jencia Tuff showing field measurements of lineated pumice and one magnetic anisotropy of susceptibility azimuth cone of confidence (95% level). Paleomagnetic sample numbers are shown with each anisotropy azimuth.

(1976) report thicknesses in excess of 650m. The unit, exposed only in the southeast part of the study area, is best exposed along the walls of East Red Canyon and Drift Fence Canyon. The base is a moderate-orange-pink crystal-poor unwelded bedded tuff (10-20m thick) that contains 5% small (<2cm) lithics. Abruptly overlying this unwelded interval is a thin (0.5m) pale red vitrophyre which marks the base of the welded Vicks Peak Tuff.

The Vicks Peak Tuff is at least 215m thick in the southeast corner of this study area. Here the base is unexposed. To the north, it thins to about 120m just east of Horse Mountain (NW1/4 sec. 27, T6S, R5W). Farther north, because of a pre-Lemitar Tuff unconformity, the Vicks Peak Tuff is rarely preserved, and its original thickness is not known.

In the southeast corner of the study area, foliation in the Vicks Peak Tuff steepens and becomes irregular and folded along a linear zone that trends about N70E (Plate 1). To the east, the zone is 500m wide, and shows a progressive increase in dip from 30 degrees in the north to >70 degrees in the south. Farther south the zone ends abruptly, and dips return to the regional trend of 10 to 15 degrees east. The structure becomes narrower (200m wide) to the west, where it crosses East Red Canyon. Here the tuff is contorted into a series of north-verging asymmetric folds

whose axial planes are mostly vertical. From north to south across the structure, the folds become tighter (nearly isoclinal), and their wavelengths decrease from about 20m to 5m. Farther to the west (sec. 4, T7S, R5W) the structure dies out completely. Apparently the Vicks Peak Tuff slumped over a south-facing scarp such as a south-side down fault, or the buried north wall of a paleocanyon while it was still hot and plastic, perhaps even during deposition. There is evidence 4km to the south, in Cold Spring Canyon, for paleocanyons of similar age (Osburn, 1982), however, the structure in this study area is not thought to be caused by a paleocanyon, because there is no evidence of a paired southern wall. Cross sections (Plate 2,3) through this part of the study area show the author's preferred interpretation of this structure.

To the west along strike of this buried escarpment, where Drift Fence Canyon turns sharply to the west (Plate 1), there is evidence for westward thickening of the Vicks Peak Tuff. The unit thickens from about 200m at the bend in the canyon to at least 300m upstream and to the south where the canyon first enters the study area (about 1.5km to the west). There is no evidence for folding of the Vicks Peak Tuff in this area.

Petrography

Distinct ledges in the Vicks Peak Tuff, along the steeper walls of East Red and Drift Fence Canyon, are thought to mark the bases of individual flow-units. The ledges, which separate continuous sequences of tuff (2-20m thick), are more deeply eroded intervals (1-50cm thick) which may represent actual cooling breaks. Alternatively, basal shear layers (layer 2a of Sparks, 1976) of flow-units in a simple cooling-unit may also account for the ledges. One of the most distinct ledges, a clast-supported lithic-tuff interval (0.5m thick), occurs about 65m above the base of the unit near the mouth of Drift Fence Canyon. The lithics in this layer, unlike those throughout the unit, are distinctively non-volcanic in origin. Lithologies in the layer (listed in order of abundance) are:

- 1) medium-grained biotite-rich monzogranite;
- 2) medium-grained sandstone;
- 3) limestone;
- 4) dark colored pieces of a garnet encrusted iron skarn.

The granite clasts are similar to those found in nearby lithic breccias of the younger South Canyon Tuff. The skarn fragments are similar to an iron skarn described by Jahns (1944) in the north end of the Sierra Cuchillo (30km to the southeast). Instrumental neutron activation analysis shows that a skarn fragment (S-37) from this study area contains 89% iron (calculated as FeO), 490ppm cobalt, and about 20ppm chromium, and tungsten.

Pumice content in the Vicks Peak Tuff increases gradually upward (2-15%). The increase, however, is irregular because individual flow-units tend to concentrate pumice in their upper parts. Most pumice fragments throughout the Vicks Peak Tuff have an internal lineation defined by elongate rods (<1mm in diameter) composed of vapor phase minerals. In the lower third of the unit, flattened pumice fragments (compaction ratios of 10:1) are mostly equant in plan view and, although internally lineated, rarely define a preferred orientation (Fig. 6a). In the southeast corner of the study area the upper two thirds of the unit contains flattened and elongated pumice fragments, up to 30cm long, with compaction ratios commonly >30:1 (Fig. 6b). Field azimuth measurements of elongated pumice in this unit are plotted in Figure 7.

The zonation of phenocrysts, pumice, and lithics in the Vicks Peak Tuff was studied in a vertical series of 8 hand specimens and thin sections (VP-1,3,5 and 85-2, to 85-2,3,4,5,6, Fig. 8). Matrix of the welded tuff, light-brownish-gray to very-light-gray in color, is usually completely devitrified to very fine grained (<0.02mm) K-feldspar. Glass shards (up to 0.5mm long) with compaction ratios of 7:1 were preserved only in the lowermost sample (VP-1), where they compose 40% of the matrix. Phenocryst content in the Vicks Peak Tuff increases from 0.5% at the base to about 2% at 70m above the base. From 70m to 100m

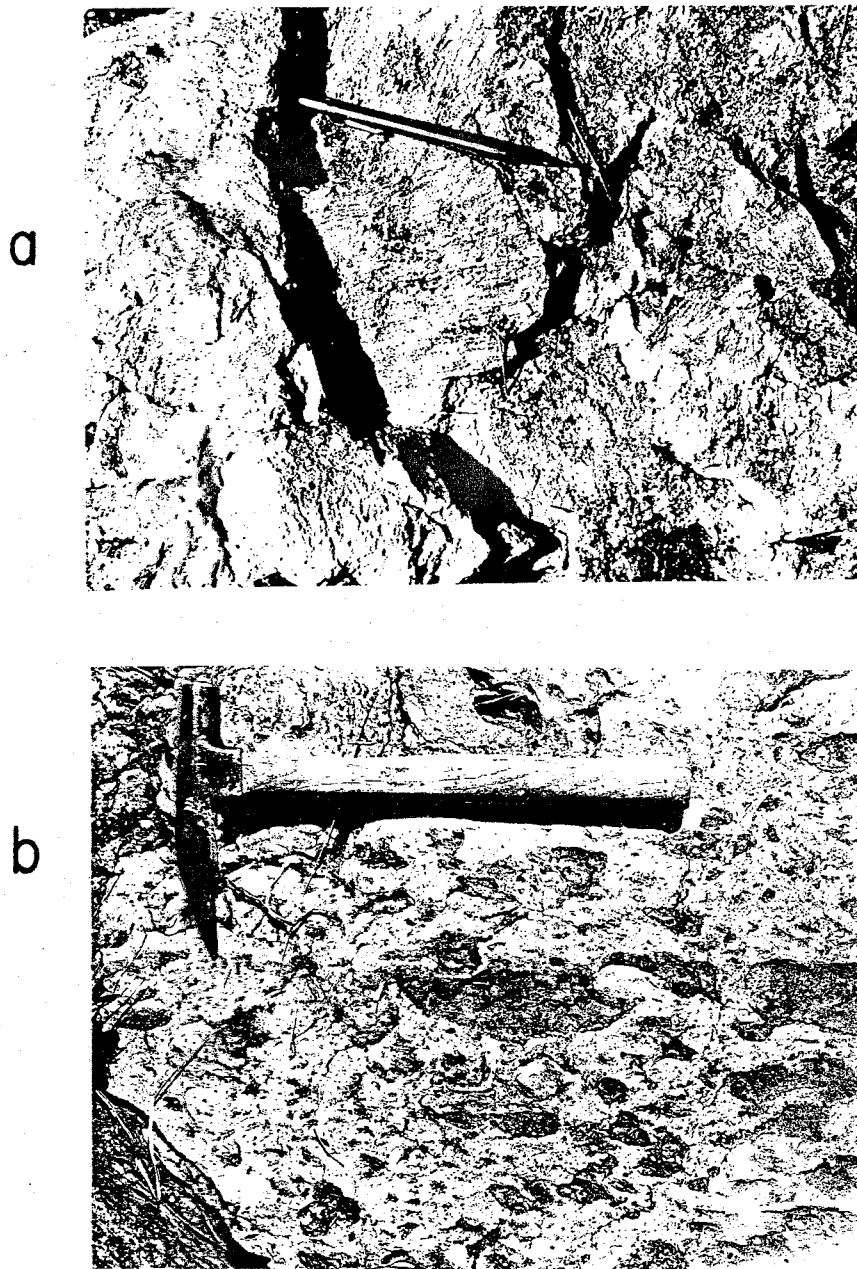


Figure 6. Photographs of lined pumice in the Vicks Peak Tuff: (a) internally lined, not preferentially oriented (sec. 6, T7S, R5w); (b) lined and preferentially oriented (sec. 4, T7S, R5W).

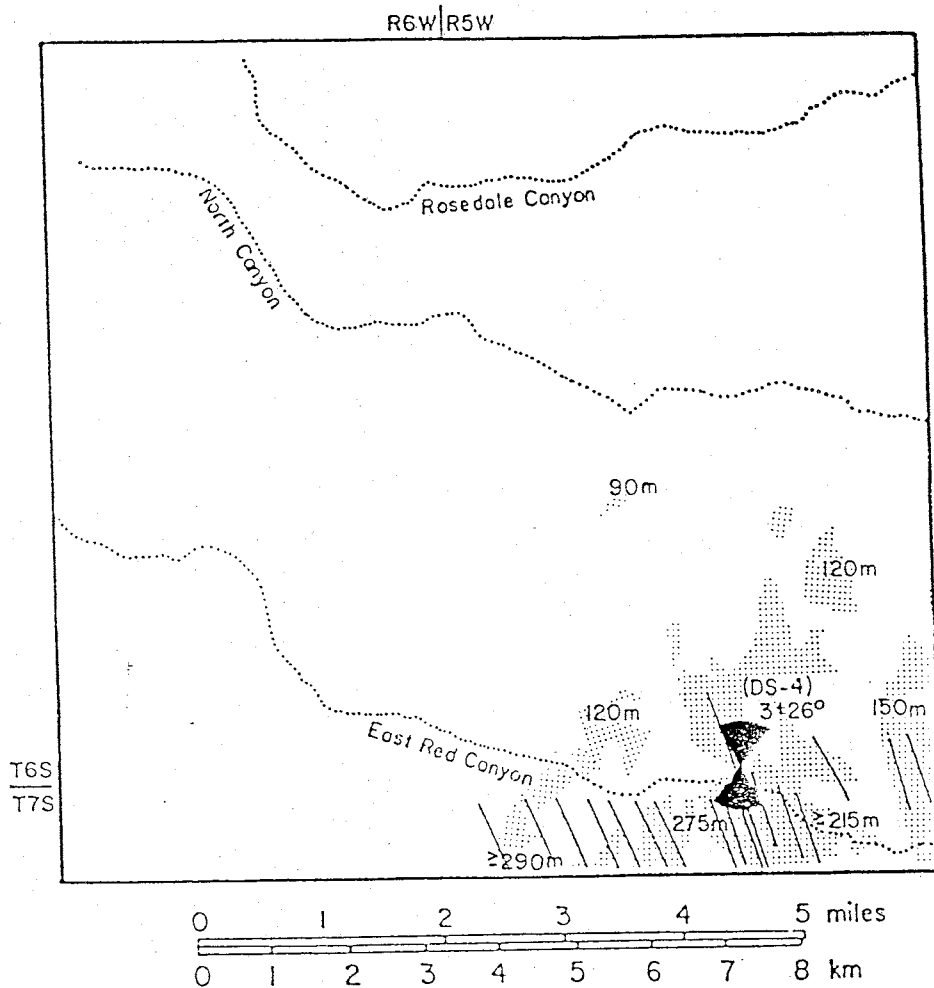
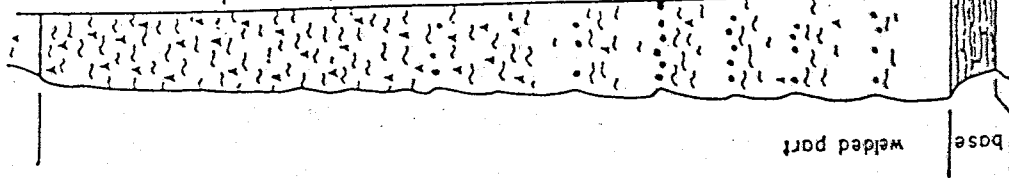


Figure 7. Outcrop map of the Vicks Peak Tuff showing thicknesses of the unit in meters, field measurements of lined pumice, and one anisotropy of susceptibility azimuth cone of confidence (95% level). Paleomagnetic sample numbers are shown with each anisotropy azimuth.

Thickness
meters
215



Sample no.	Color unweathered matrix	Lithics	Pumice	Total phen.	San.	Qtz.	Plg.	Biol.	Opaa.	Cpx
85-6	brownish-gray 5YR 4/1	t	12-20	12	12	0	0	0	t	m
85-5	brownish-gray 5YR 5/1	t	8-12	10	10	0	0	0	t	t
85-3	medium-gray N 6	t	4-8	9	9	0	0	0	t	t
85-4	light-brownish-gray 5YR 6/1	t	4-8	2	2	0	0	0	t	t
85-2	light-gray N 7	t	4-8	2	2	t	t	t	t	t
VP-5	light-gray N 7	t	4-8	1.5	1.5	0	t	t	t	t
VP-3	light-gray N 7	t	4-8	1	1	t	t	t	0	0
VP-1	light-brownish-gray 5YR 6/1	1-2	3	0.5	0.5	0	0	t	0	0
0	m-minor (less than 0.5%)	t-trace (less than 0.1%)						0-not observed		

(22)

~ Pumice fragments

•• Lithic fragments

▲ Phenocrysts

Figure 8. Stratigraphic section of the Vicks Peak Tuff (sec. 4, T7S, R5W). Visual estimates of phenocryst percentages are from thin sections, and lithic and pumice percentages are estimated from hand specimens.

above the base, phenocryst content increases from 2% to 10%, and then to about 12% at the top (215m). Phenocrysts throughout the unit are dominately tabular euhedral sanidine (1-4mm). Small phenocrysts (<0.5mm) of quartz, plagioclase, and biotite occur in trace amounts in the lower 100m of the unit. Rounded opaque grains (<0.5mm), and subhedral tabular clinopyroxene (0.2-1.0mm) occur in trace to minor amounts in the middle to upper part of the unit.

Tuff of The Park

Distribution

The tuff of The Park (new informal name), a light-gray moderately welded rhyolite ash-flow tuff, is the oldest unit exposed in the western part of the study area (Fig. 9). The unit's base is not exposed in the study area, but it is at least 60m thick near The Park (NW1/4 sec. 26, T6S, R6W).

The tuff of The Park is intruded by the rhyolite of Exter Canyon. Subsequently, both units were uplifted, eroded, and buried by 40-70m of Lemitar Tuff. In The Park area, a slight angular unconformity (15 degrees) occurs between the Lemitar Tuff and the tuff of The Park. In the Allen Spring area, the tuff of The Park is overlain by cross-stratified sandstones of the unit of East Red Canyon. Structural attitudes in the unit could not be obtained here

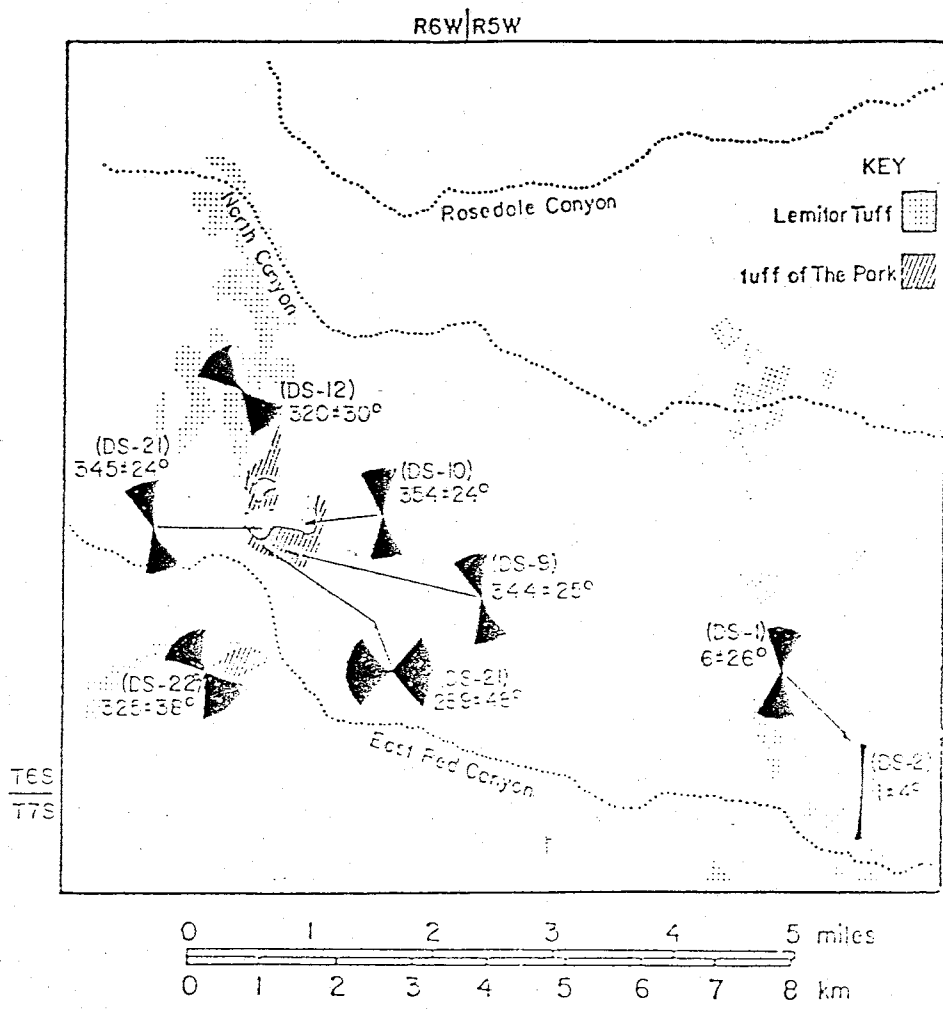


Figure 9. Outcrop map of the tuff of The Park (lined pattern) and the Lemitar Tuff (stippled). Magnetic anisotropy of susceptibility azimuth cones of confidence (95% level) for both units are also plotted. Paleomagnetic sample numbers are shown with each anisotropy azimuth.

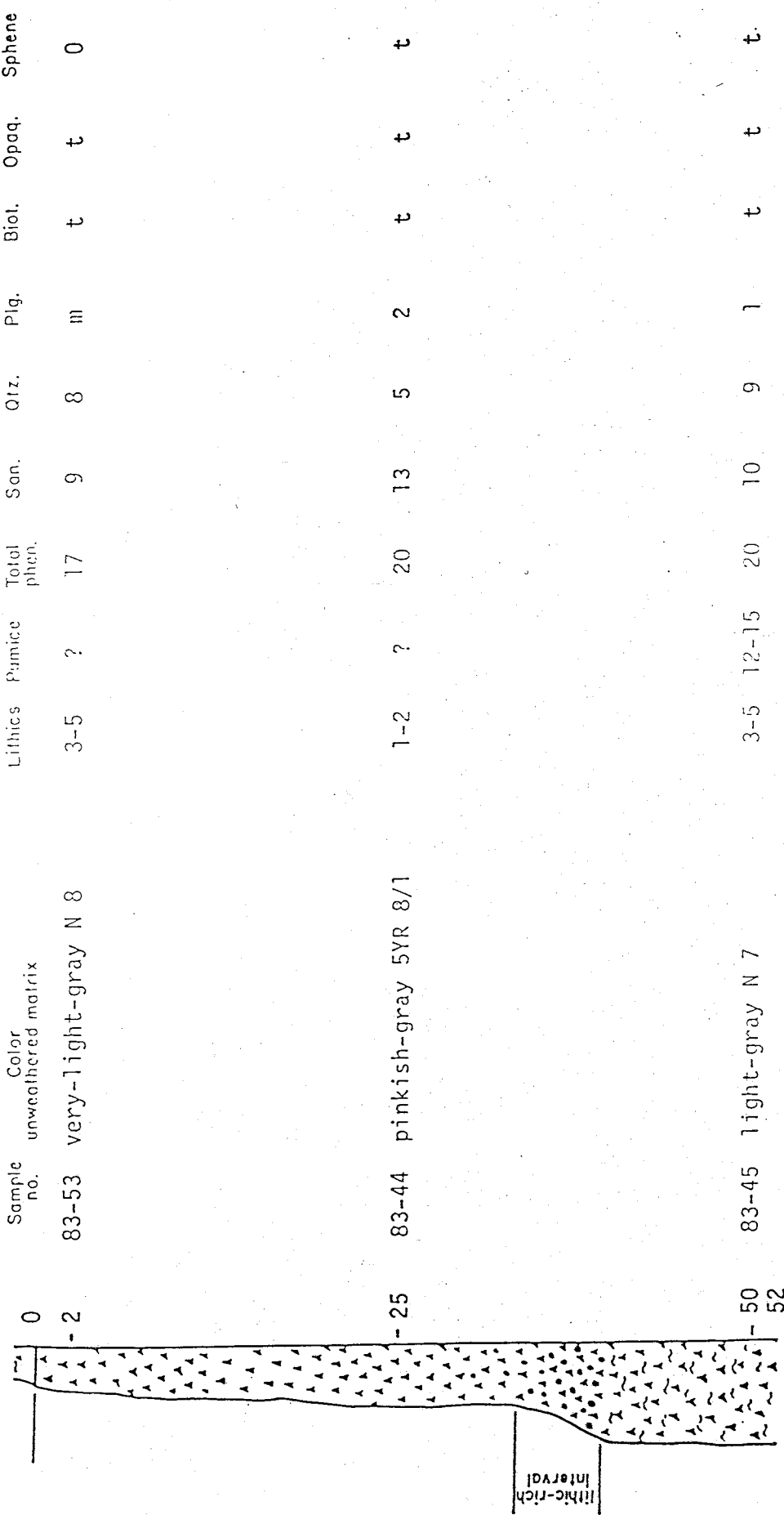
because pumice could not be recognized.

Petrography

Thin sections were studied from samples collected 25m (83-44) and 50m (83-45) below the top of the unit at The Park. Another thin section (83-53) was studied from the top of the unit in the Allen Spring area (1km south). It is not certain exactly how the top of the unit correlates between these two locations. The unit consistently contains about 18-20% phenocrysts consisting of subequal amounts of quartz (1-2mm) and sanidine (1-2mm), and 1-2% plagioclase (0.5mm). The unit also contains trace amounts of biotite (0.3mm), sphene (0.3mm), and opaque minerals (0.3mm). The concentration of phenocrysts, pumice and lithics in this unit is summarized in Figure 10.

There is a prominent lithic-rich interval (5m thick) that starts approximately 40m below the top of the unit (Fig. 10). Lithic fragments (<20cm), composing about 10% of the tuff here, consist of rhyolite and basaltic andesite lava and a distinctive moderate-red crystal-rich ash-flow tuff. There is no evidence of a cooling break near this lithic interval; however the degree of welding is less above than below. Below the lithic zone, the tuff is moderately to densely welded with pumice that have compaction ratios of 5:1. Glass shards can still be

Thickness
meters



m-minor (less than 0.5%) t-trace (less than 0.1%) 0-not observed

~ Pumice fragments

•• Lithic fragments

▲ Phenocrysts

Figure 10. Stratigraphic section of the tuff of The Park (sec. 23, T6S, R6W). Visual estimates of phenocryst percentages are from thin sections, and lithic and pumice percentages are estimated from hand specimens.

recognized in thin section, even though the matrix is mostly devitrified. All of the tuff above the base of the lithic zone is poorly welded, and pumice are very difficult to recognize. In thin section the matrix of this upper interval is thoroughly devitrified. The devitrified matrix contains irregular shaped clots (1mm) defined by slightly larger microcrystals (quartz and sanidine), and by a higher concentration (3 times the rest of the matrix) of opaque oxide blebs (<0.2mm).

First stage rhyolites

Rhyolite lava of Drift Fence Canyon

DISTRIBUTION

The rhyolite lava of Drift Fence Canyon consists of at least one plug, a set of north-northwest trending dikes, and at least two flows that intrude or overlie the Vicks Peak Tuff. The upper age of the unit is constrained by two small outcrops of Lemitar Tuff that fill a paleocanyon cut through into the base of the oldest lava flow. The plug(s) and dikes are the source of at least two flows, with a composite thickness of at least 70m, that extend about 1.6 km to the north and south of East Red Canyon (Plate 1).

Eruptive centers for the Drift Fence Canyon lavas form a linear array that trends about N20E, but the orientation of individual feeder dikes trends about N30W (Fig. 11). The phenomenon of en-echelon feeder dikes along linear arrays of silicic domes has been discussed by Fink (1984) for the Inyo Volcanic Chain, Long Valley Caldera, California. Fink suggests that at depth, magma propagates along established joints and fractures, but near the surface (intruding younger rocks) it propagates along dikes whose trends reflect regional stress patterns. The dikes of the rhyolite of Drift Fence Canyon fit this pattern. The aligned eruptive sites for the Drift Fence Canyon rhyolites parallel local Basin and Range faults, whereas the individual feeder dikes trend northwest, perpendicular to the least principle stress direction (Fig. 11).

Almost all of the Drift Fence Canyon lava flows were eroded to the north and east of the vent area. The remaining outcrops of these lavas formed a divide between two north-northeast trending paleocanyons that were subsequently filled with the Lemitar Tuff (Fig. 12). Younger deposits to the southwest bury evidence of the unit's westward extent, and only a small remnant of the unit is preserved to the east (NE1/4 sec. 33, T6S, R5W).

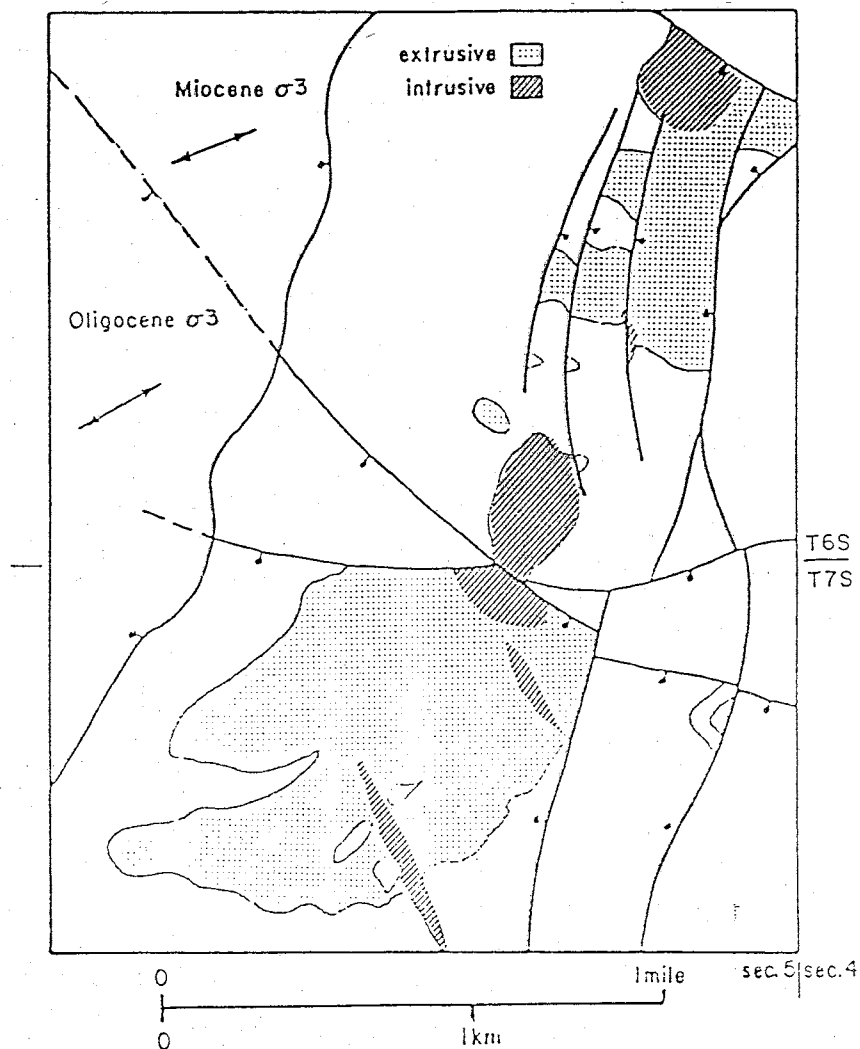


Figure 11. Outcrop map of the rhyolite lava of Drift Fence Canyon, see text for discussion. The Miocene $\sigma 3$ is from Zoback and others (1981), and the Oligocene $\sigma 3$ is from this study (see Table 3).

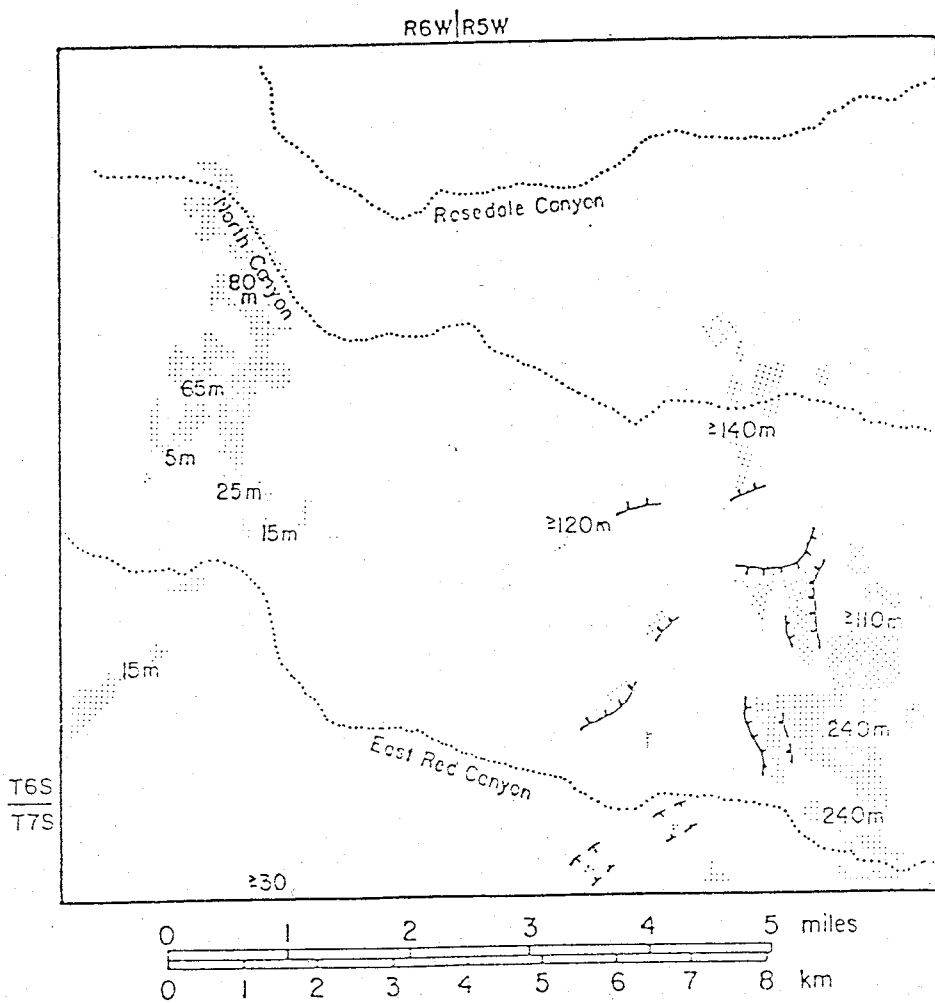


Figure 12. Outcrop map of the Lemitar Tuff showing thicknesses in meters and the distribution of paleocanyon walls buried by the unit.

PETROGRAPHY

The rhyolite lava of Drift Fence Canyon (sample 85-7) contains 5-10% phenocrysts of euhedral blocky sanidine (1mm), and subhedral blocky plagioclase (1mm) in subequal proportions. Subhedral resorbed quartz (1mm), biotite (0.5mm), and opaque minerals (0.3mm) occur in trace amounts.

Rhyolite of Exter Canyon

DISTRIBUTION

The rhyolite of Exter Canyon, exposed along the western edge of the study area, intrudes the tuff of The Park, and is unconformably overlain by the Lemitar Tuff. The unit's outcrop pattern between East Red Canyon and Exter Canyon suggests that it is an eroded intrusive plug.

PETROGRAPHY

In thin section, the rhyolite of Exter Canyon (84-159) contains 10% phenocrysts of euhedral blocky sanidine (1-2mm), and euhedral blocky plagioclase (1-2mm) in subequal proportions. Both feldspars are almost completely altered to clay minerals. Biotite, which occurs in trace amounts, is altered to opaque minerals and highly birefringent material that is probably a mixture of epidote and zoisite.

Lemitar Tuff

Distribution

The Lemitar Tuff (Osburn, 1978) is a crystal-poor to crystal-rich rhyolite ash-flow tuff. In the western part of the study area, it rests with slight angular unconformity on the rhyolite of Exter Canyon and the tuff of The Park, and is overlain by the South Canyon Tuff. In this part of the study area the Lemitar Tuff thickens from 5-15m in the south to about 80m in the north.

In a north-south band across the middle of the study area, except for one exposure (at least 30m thick) underneath the Cave Peak dome, the unit is unexposed. About 1km to the northwest (in the Allen Spring area), sandstones younger than the Cave Peak dome overlie the tuff of The Park, and the Lemitar Tuff is not preserved.

Throughout the southeast part of the study area, the Lemitar Tuff is intruded by second stage rhyolites. It is overlain by unwelded crystal-poor bedded tuffs of the unit of East Red Canyon in the North Canyon area, and by unwelded South Canyon Tuff in the extreme southeast corner of the study area. Throughout the southeast part of the study area, the Lemitar Tuff fills paleocanyons that cut into Vicks Peak Tuff, and in some places into the La Jencia Tuff (Fig. 12). These paleocanyons, which trend north-south or

northeast-southwest, attain maximum depths of about 150m, and widths of about 400m. Outside of these paleocanyons, the unit is about 200m thick.

Petrography

The Lemitar Tuff is a pale-red to reddish-brown densely welded tuff except for its base which is poorly welded and a gray-orange-pink color. Phenocryst content in the unit increases continuously upward from 6-8% at the base to 40% at the top. Pumice content also increases upward from less than 1% at the base to about 10% at the top. Pumice fragments rarely exceed 10 cm in length (average 3-5cm), and compaction ratios are usually <10:1. There is no indication of elongation or lineation of the fragments. Lithic fragments rarely exceed 5% of the tuff, and are usually <2cm in diameter. They are most abundant (5-10%) at the base of a distinctive quartz-poor interval in the lower half of the unit. Lithic fragments in this interval are mostly rhyolitic or andesitic lava, but there are also minor amounts of crystal-rich fragments that are petrographically similar to the upper crystal-rich part of the Lemitar Tuff.

The vertical zonation of phenocrysts in the Lemitar Tuff is its single most diagnostic feature. A series of 6 samples (83-110, 84-160 to 84-164) was studied from a 80m thick section measured on the west side of North Canyon in

the western part of the study area (Plate 4). Petrographic data from the section in this study area (Fig. 13) correlates well with a section of the Lemitar Tuff in the Magdalena Mountains described by Osburn (1978). The unit's base contains 6-8% small (1mm) broken phenocrysts of sanidine, quartz, minor plagioclase, and a trace of biotite. The small size and broken nature of the phenocrysts continues up through the lower third of the unit to where a distinctive quartz-poor interval starts. This interval, about 12 meters thick here, is characterized by low quartz content (1-2%), and an increase in the average size of the feldspar grains (2-4mm). Also in the interval, there is an increase in plagioclase (10%), and biotite (1-2%). Above this interval quartz becomes larger (2-4mm), deeply resorbed, and more abundant (10%). Also above the interval, biotite decreases to <1%, but plagioclase increases to about 15%. At the top of the unit, plagioclase decreases to about 5%, and clinopyroxene (<0.2mm) occurs in trace amounts. Throughout the unit, euhedral sanidine (0.5-4mm) composes at least half the phenocrysts.

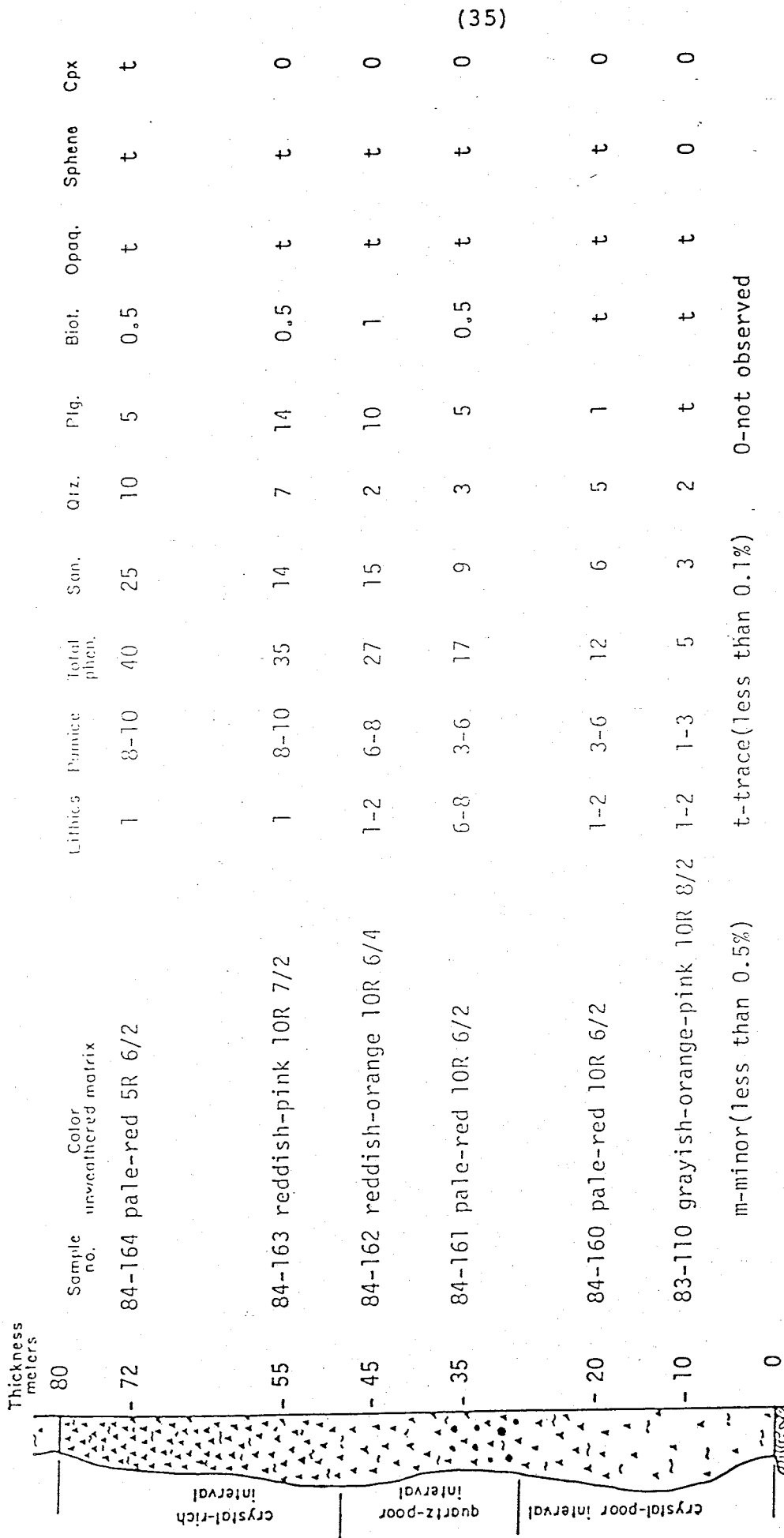


Figure 13. Stratigraphic section of the Lemitar Tuff (sec. 11, T6S, R6W). Visual estimates of phenocryst percentages are from thin sections, and lithic and pumice percentages are estimated from hand specimens.

- ~ Pumice fragments
- Lithic fragments
- ▲▲ Phenocrysts

Second Stage Rhyolites

Distribution

There are 10 separate occurrences of rhyolite lava flows, plugs and dikes in this study area that are thought to be younger than the Lemitar Tuff, and older than the South Canyon Tuff. The ages of most of these rocks, however, can not be precisely constrained relative to both tuff units. Most of the rhyolites clearly intrude or overlie the Lemitar Tuff, but only a few are overlain by the South Canyon Tuff or the unit of East Red Canyon. Each occurrence of rhyolite is located, and given an unofficial name on Plate 1.

Most of the second stage rhyolites were intruded along a north-northeast trending west-side down structural zone (about 2km wide) that extends across the study area (Plate 1). To the west of this structure, lavas are overlain by younger deposits, but to the east of it, intrusive levels are exposed, revealing the shapes of the plugs and dikes (Plate 1). The plugs and dikes here, elongated in a north-south direction, are bisected by a series of south-side down faults which expose successively deeper stratigraphic levels to the north. In the north, rhyolite is exposed as north-trending anastomosing dikes, but to the south it occurs as elongate plugs. Farther south, at higher

stratigraphic levels, the plugs are more cylindrical in shape.

Intrusive plugs and dikes of the second stage rhyolites are typically strongly flow-banded, and foliation is near vertical. In some of the larger plugs, cooling joints up to 0.5m in diameter occur oriented perpendicular to the dominant plane of flow-banding, and to intrusive contacts. The only extensive lava flow in the southeast part of the study area is the lava of Horse Mountain Canyon. This lava is usually fairly brecciated, and rarely flow-banded. It was not possible to define individual flows, determine thicknesses, or to identify any vents in this area.

Petrography

In hand specimen, the second stage rhyolites are light-gray to light-brownish-gray, and contain 3-10% phenocrysts of feldspar and quartz. The quartz to feldspar ratio in these rocks ranges from 1:1 to 1:6. The only sample studied in thin section, the rhyolite of Horse Mountain (83-32), contains 6% phenocrysts of blocky euhedral sanidine (1-2mm), blocky subhedral quartz (1-2mm), and blocky subhedral plagioclase (1mm) in an approximate 2:2:1 ratio. Quartz is slightly resorbed, and plagioclase is commonly glomeroporphyritic. Biotite (0.3mm), opaque minerals (0.2mm), and euhedral sphene (0.3mm) occur in trace

amounts.

Unit of East Red Canyon

Distribution

The unit of East Red Canyon (new informal name) is a sequence of epiclastic and minor pyroclastic rocks that is younger than the Lemitar Tuff, but older than the South Canyon Tuff. All epiclastic rocks in this unit contain at least 50% volcanic rock fragments and can be classified as volcanoclastic. The base of the unit overlies eroded plugs and lava flows of second stage rhyolites in the southern part of the study area, but to the north the age relationship between the unit and second stage rhyolites is poorly constrained. The unit of East Red Canyon was deposited in a north-northeast trending basin, 5 km across, that extends 5 km into the study area from its southwest corner (Fig. 14). The basin is bounded on the northwest by an east-side down fault, and on the southeast by a post-Lemitar west-side down fault and or monocline. North of East Red Canyon, the basin may continue underneath the South Canyon Tuff or terminate against a south-side down fault. To the south, basin sediments lap onto the north face of a large (3km diameter) second stage rhyolite dome (Cave Peaks). To the southwest, the basin continues into unmapped terrane.

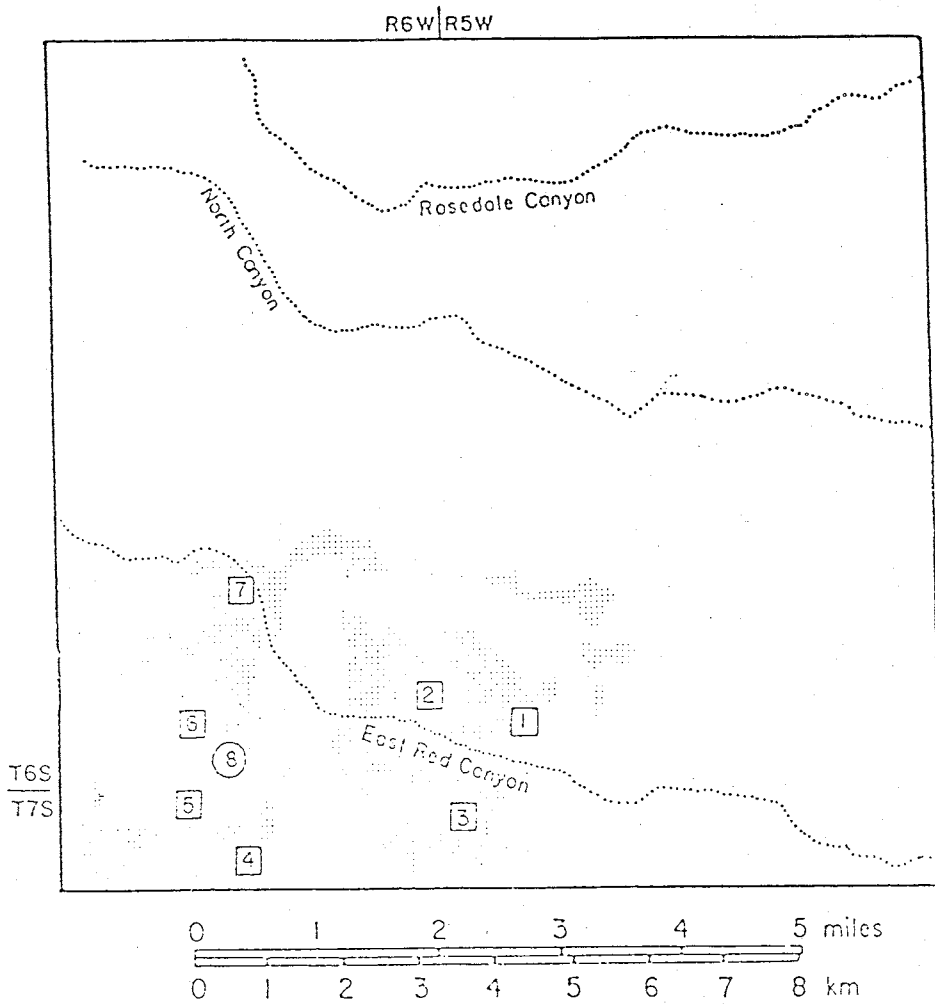


Figure 14. Outcrop map of the unit of East Red Canyon showing the location of the measured sections described in Figure 15a,b.

Within the basin, underlying volcanic rocks are exposed in only three places (Plate 1). The unit of East Red Canyon is about 200m thick in the Allen Spring area, but the base is otherwise unconstrained throughout most of the basin, and greater thicknesses are possible. Outside of its structural basin, the unit is rarely exposed. About 20-30m of the unit overlies second stage rhyolites just to the east of the basin's margin (sec. 29,32, T6S, R5W). One small exposure of sandstone underlies the South Canyon Tuff just north of the basin (sec. 19, T6S, R5W). In North Canyon about 50m of bedded tuffs and minor epiclastic rocks, correlated with the upper part of the unit, conformably overlie tilted blocks of Lemitar Tuff.

Petrography

Six generalized stratigraphic sections (located in Fig. 14) of the unit of East Red Canyon were measured throughout the basin. One detailed section was described from a sequence of cross-stratified sandstone in the western part of the basin. Lithologies in the stratigraphic sections (Fig. 15a,b) are listed and briefly described below.

Clast-supported diamictite occurs in 0.3 to 3.0m thick beds that have sharp, but usually non erosional, lower contacts. The clasts (<1cm-3.0m), cemented in a medium to fine-grained matrix, are subangular to subrounded. The

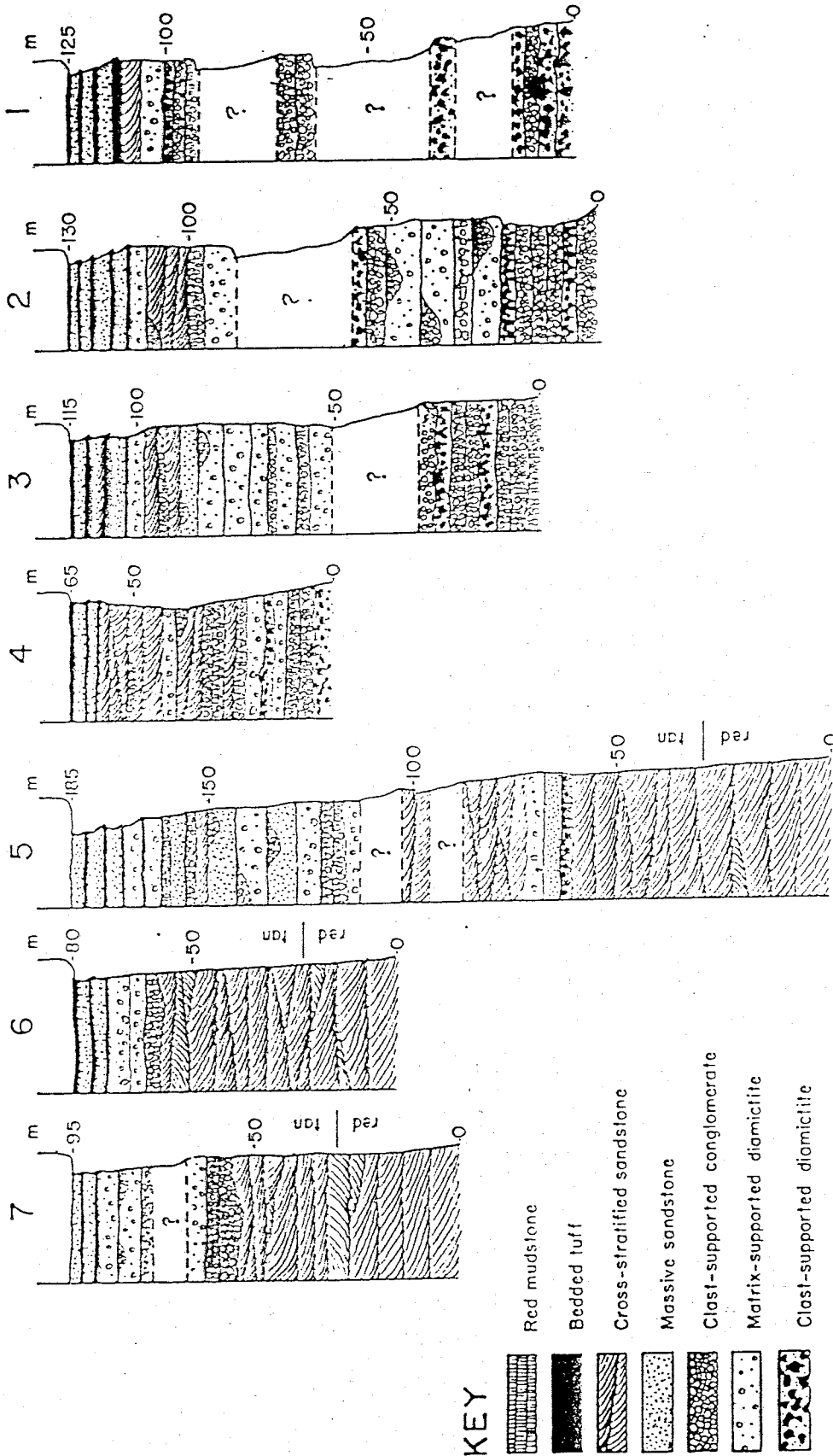


Figure 15(a). Generalized stratigraphic sections of the unit of East Red Canyon.

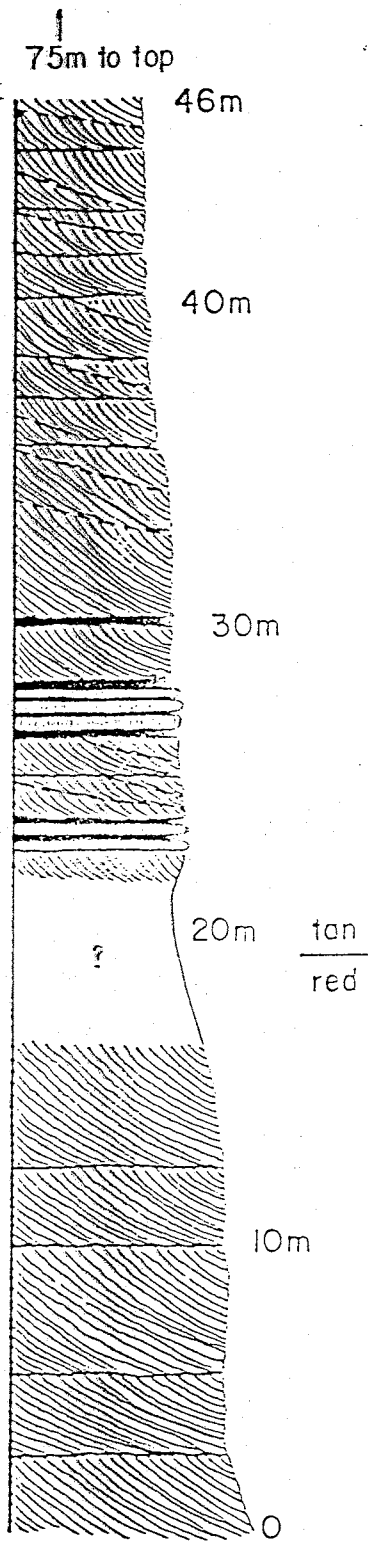


Figure 15(b). Detailed stratigraphic section of eolian sandstone in the unit of East Red Canyon (sec. 3, T7S, R6W).

beds, interpreted as deposits of clast-rich debris flows (Shultz 1984), are characterized by an absence of layering or sedimentary structures, except for reverse grading at their base.

Matrix-supported diamictite, interpreted as deposits of pseudoplastic debris flows (Shultz, 1984), occur in beds (0.5-5.0m thick). They contain 5-20% clasts (0.5-10.0cm) suspended in matrix-supported sandstone (Fig. 16). The base of the beds are typically coarser grained, and may be clast-supported.

Clast-supported conglomerate, interpreted as stream-channel or sheetflood deposits, is the most abundant coarse-clastic lithology in the basin. It occurs in lenticular to tabular 0.1 to 2.0m thick sets that usually have sharp lower contacts. Clasts (<1cm to 30cm) are sub-rounded to rounded, and are arranged in bedded sets that are usually normally graded.

Massive sandstone occurs in beds 0.5-6.0m thick composed of medium to coarse-grained, moderately well to poorly-sorted sandstone. Lower and upper contacts may be sharp or gradational with adjacent units. The sandstone may contain up to 15% pumice fragments that are 5 to 10 times larger than the median grain size.



Figure 16. Photograph of matrix supported diamictite (sec. 3, T7S, R6W).

Cross-stratified sandstone occurs in planar tabular to wedge-shaped sets 0.5-7.0m thick. The medium to fine grained sand is moderately well-sorted to very-well sorted, and is deposited in extremely continuous cross-strata that dip from 2 to 35 degrees (Fig. 17). The sandstones are thought to be eolian partly because the scale of cross-strata sets (up to 7.0m thick) is too great to be realistically compared with any non-eolian terrestrial environment. The most diagnostic eolian characteristic of the sandstones, however, is the widespread occurrence of the three basic types of eolian stratification; grainfall; grainflow; and wind-ripple laminae (Hunter, 1977). Grainfall deposits, the most abundant stratification type observed in this study area, are thin blanket-like laminae that accumulate on the lower lee-slopes of dunes. Grainflow deposits, lenticular bodies of sand that have avalanched down over-steepened dune faces, are usually found on the upper lee slopes of dunes, and therefore are rarely preserved. Grainflow deposits are rare, but do occur in the upper part of the thickest cross-strata sets in this study area. Eolian rippleform laminae commonly form on windward slopes, reactivation surfaces, and the lower lee slopes of dunes. Rippleform laminae from this area are identified as eolian because of their high (>15) ripple indices (wavelength divided by the height).



Figure 17. Photograph of basal portion of a cross-stratified sandstone set (sec. 26, T6S, R6W).

An important feature of cross-stratified sandstone in the unit of East Red Canyon is laterally extensive planar erosion surfaces that bound the sets. Brookfield (1977) recognizes three orders of bounding surfaces with higher (first) order surfaces truncating progressively lower (second and third) order surfaces. First order surfaces represent interdune deflation areas that have been buried by migrating complex dunes or draas. Second order surfaces separate individual dunes that migrate across the complex dunes, and third order surfaces are reactivation surfaces within these dunes. In the detailed stratigraphic section of cross-stratified sandstone (Fig. 15b), first and second order surfaces are delineated with solid and dashed lines, respectively. Third order surfaces are too subtle to be shown here. Figure 18 is a photograph of a cliff of eolian sandstone illustrating typical first order surfaces in this study area. Figure 19 is a schematic block diagram showing migrating eolian bedforms that may account for these bounding surfaces. In Figure 19, the interdune deflation areas, when buried by the next dune system, become first order bounding surfaces.

Bedded Tuff occurs in 0.2-2.0m thick sets of crystal-poor unwelded thin-bedded to very thin-bedded ash-fall tuff, ash-flow tuff and possible surge deposits (Fig. 20). Red mudstone occurs as 2-5cm thick beds of red mudstone which commonly show desiccation cracks (Fig. 21).

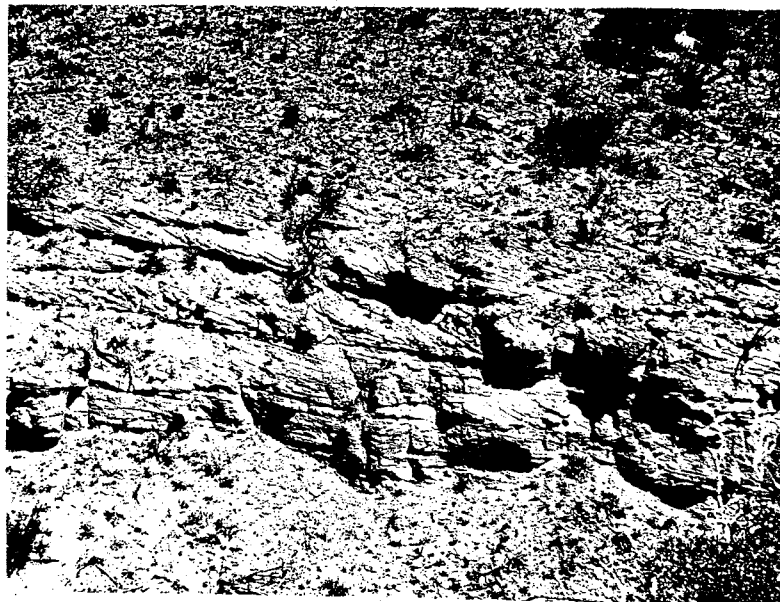


Figure 18. Photograph of cliff of eolian sandstone (cliff is about 20 meters high) illustrating typical first order bounding surfaces (sec. 26, T6S, R6W).

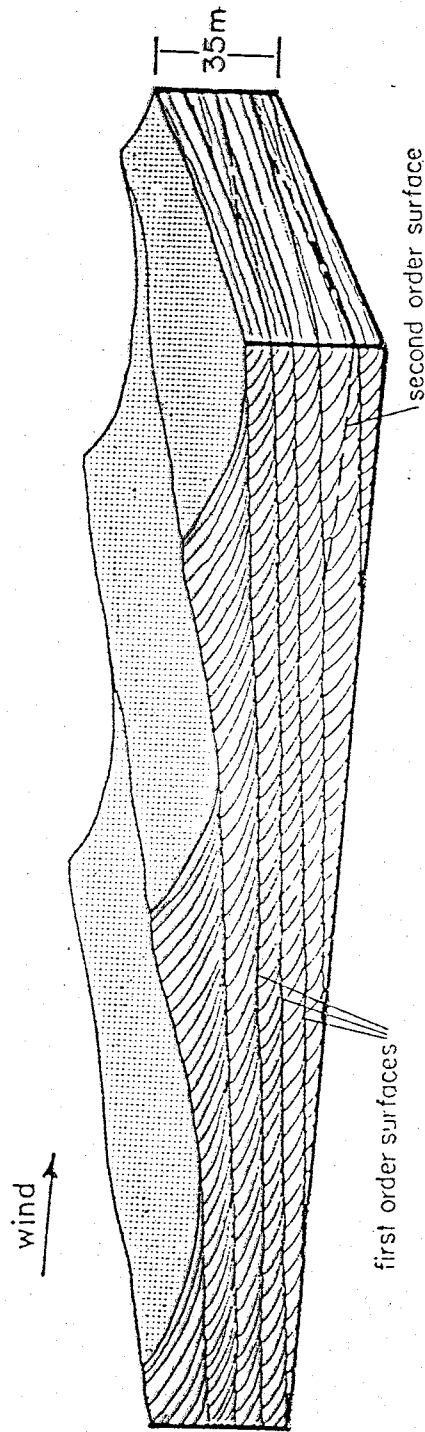


Figure 19. Block diagram showing a possible origin of the first order bounding surfaces observed in the unit of East Red Canyon.



Figure 20. Photograph of a 1 meter thick sequence of bedded ash-flow tuff (sec. 35, T6S, R6W).



Figure 21. Photograph of desiccation cracks in a mudstone bed (sec. 26, T6S, R6W).

Stratigraphic sections

The stratigraphic sections (Fig. 15a,b) indicate different depositional histories for the east and west parts of the unit of East Red Canyon. The only consistent part of the unit throughout it's basin is the upper 10-30m, which consists of massive-sandstone and cross-stratified sandstone interlayered with sets of bedded-tuff.

The eastern part of the basin, interpreted as an alluvial fan complex, consists mostly of clast-supported diamictite and clast-supported conglomerate which grade upward into sandstones in the upper 20-30m of the unit. Coarse-clastic detrital fragments here consist of 90% rhyolite lava and about 10% crystal-rich rhyolite ash-flow tuff which could be the Lemitar Tuff. Paleocurrent directions were not measured here because imbrication or cross-stratification was not recognized. However, because of an overall decrease in the average size, and increase in textural maturity of the sedimentary grains from east to west, It is likely that the southeast margin of the basin was a major source of sediment for this fan complex.

The transition from coarse-clastic dominated lithologies in the east to sandstone dominated lithologies in the west is obscured by a north-south trending structural graben that transects the basin. Rocks in the western part of the basin consist mostly of cross-stratified eolian

sandstone. The lower 60-100m of these sandstones are red colored, but above they are light-tan or buff colored. In Figure 15b, this color change occurs just below a sequence of bedded tuffs and red mudstones. The mudstones probably formed just above a permanent water table in interdune deflation areas that were periodically wet. Sediment below this paleo water table may have been oxidized and stained red before the upper light colored sand was deposited. One thin section (83-300) of the lower red sandstone, and two thin sections (83-51,207) of the upper light colored sandstone were studied and point-counted (Table 1). The sandstones are composed primarily of rhyolitic lithic grains (55-75%), but also contain significant amounts of basaltic lithic grains. A rose diagram of paleocurrent measurements in eolian sandstones throughout the unit of East Red Canyon is plotted on Figure 22. The northeast transport direction is typical of Cenozoic wind directions in central New Mexico (Lambert, 1968, p. 197, 211). Clast-supported conglomerate and diamictite, in the western part of the basin, are found only in the upper 30-60m of the unit (Fig. 15a) The coarse detrital fragments here consist of only about 60% rhyolite lava, and about 40% crystal-poor (Vicks Peak?) and crystal-rich (Lemitar?) rhyolite tuff.

Table 1. Percentages (determined by point-count) of grain types in eolian sandstones from the unit of East Red Canyon.

Sample	pore space	felsic volcanic lithics	mafic volcanic lithics	sanidine and quartz	plagioclase	mafic minerals	microcline	points counted
83-301	29	40	19	10	1	0.1	0.1	1638
83-207	10	68	8	9	3	1.2	0.2	1604
83-51	24	61	5	13	2	1.8	0.3	1000

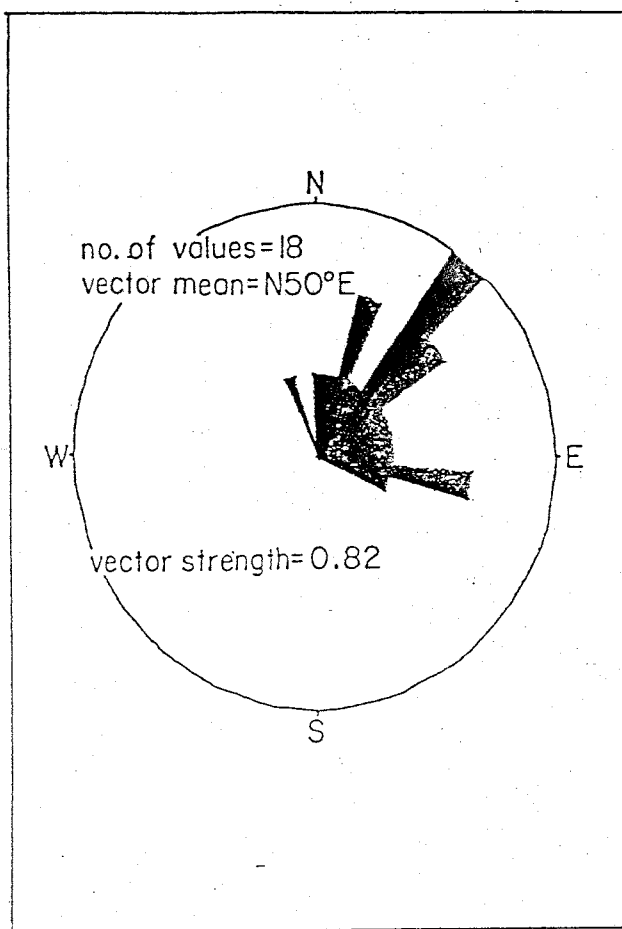


Figure 22. Rose diagram of paleocurrent directions from eolian sandstone in the unit of East Red Canyon.

Paleontology

Two kinds of ichnofossils were found in the upper part of the unit of East Red Canyon. A cast of arctiodactyl (split hooved mammal) hoof prints (Fig. 23) was found in a loose slab of bedded-tuff in Allen Spring Canyon. In the same canyon, an inclined burrow, about 6cm in diameter, was found at the top of a cross-stratified sandstone set (Fig. 24). The burrow, filled with ash below and sand above, is overlain by a 0.5m thick set of bedded tuff, which is overlain by a bed of massive sandstone. One possible interpretation is that, buried by an ash-fall layer, the burrowing animal dug it's way out, and in route to the surface pushed stoped ash to the bottom of the burrow. Eventually, the burrow filled with sand from above.



Figure 23. Photograph of arctiodactyl hoof print molds in a slab of bedded tuff (sec. 35, T6S, R6W). The pencil for scale is about 10cm long.



Figure 24. Photograph of inclined burrow about 6cm in diameter (sec. 35, T6S, R6W), see text for discussion.

South Canyon Tuff

Distribution

The South Canyon Tuff (Osburn, 1978) is a crystal-poor to moderately crystal-rich vertically zoned rhyolite ash flow tuff that is exposed over most of the northern half of the study area. The basal 20m of this unit is all that remains in the southeast corner, but it is at least 400m thick in the southwest corner, and at least 650m thick in the northern part of the study area. In the southern part of the study area, the unit rests on the Lemitar Tuff, second stage rhyolites, and the unit of East Red Canyon. In the northwest part of the study area, South Canyon Tuff rests on Lemitar Tuff, but east of here it's base is not exposed. Overlying the South Canyon Tuff in the northern part of the area, is the unit of North Canyon, and in the northeast corner the tuff of Rosedale Canyon. The unit is also intruded by the rhyolite of Wildcat Peak and associated dikes in the north-central part of the area.

Members of the South Canyon Tuff

Within this study area, five members of the South Canyon Tuff are recognized (Plate 1). These consist of: 1) welded tuff member; 2) unwelded basal member; 3) phreatic pipe member; 4) clast-supported lithic breccia member; and

5) crystal-rich member.

The welded tuff member is volumetrically the most important of the South Canyon Tuff. It consists of all welded tuff throughout the unit, including a basal vitrophyre. Also mapped with this member are poorly welded tuffs adjacent to pods of clast-supported lithic breccia.

The lowest member of the South Canyon Tuff is its 10-70m thick unwelded base. This member occurs as a mappable unit only in the sedimentary basin of the unit of East Red Canyon, and adjacent to Wildcat Peak (Plate 1). The unwelded basal member is distinguished from unwelded bedded tuffs in the upper part of the unit of East Red Canyon, because it forms a single massive unit that is continuous with the overlying welded South Canyon Tuff.

The phreatic pipe member is composed of two oval shaped vertical pipes (about 20m across) that intrude welded South Canyon Tuff near Turkey Spring (Plate 1). The pipes consist of unwelded bedded tuffs in the center, some of which may be water-laid, and massive unwelded tuff around the edges. The contact with the welded tuff is sharp, and characterized by veins of agate (<1cm thick) that invade fractures in the welded tuff. Both pipes are located adjacent to, and on the downthrown side of, a pair of graben faults in the sedimentary basin of the unit of East Red Canyon. The pipes are interpreted as phreatic explosion tubes formed over

springs or standing water along the buried fault traces.

The clast-supported lithic breccia member is restricted to an area described by a 2km radius semicircle centered on and extending to the northwest of Wildcat Peak. It consists of discontinuous pods or lenses (10-100m thick) of clast-supported lithic breccia, with unwelded tuff matrix, that grade laterally into poorly welded portions of less lithic-rich tuff. The breccias occur at various stratigraphic levels in the South Canyon Tuff, but are found mostly at the base, and near the top. Lithic fragments in this member are composed mostly of rhyolite lava or Lemitar Tuff. The average size of the largest 5 lithic fragments recorded at each exposure of this member are plotted in Figure 25. Lithic fragments are as large as 3 meters near Wildcat Peak, but they decrease in average size away from this area.

Petrography

A 100m thick vertical section of the the South Canyon Tuff, comprising 7 samples (84-4-1,7), was collected at Turkey Spring (Plate 4) for combined micropetrographic and geochemical studies. Thin sections of 17 additional samples from throughout the study area (Plate 4) were also studied. Estimates of phenocryst, pumice, and lithic content in samples from the Turkey Spring section are presented in

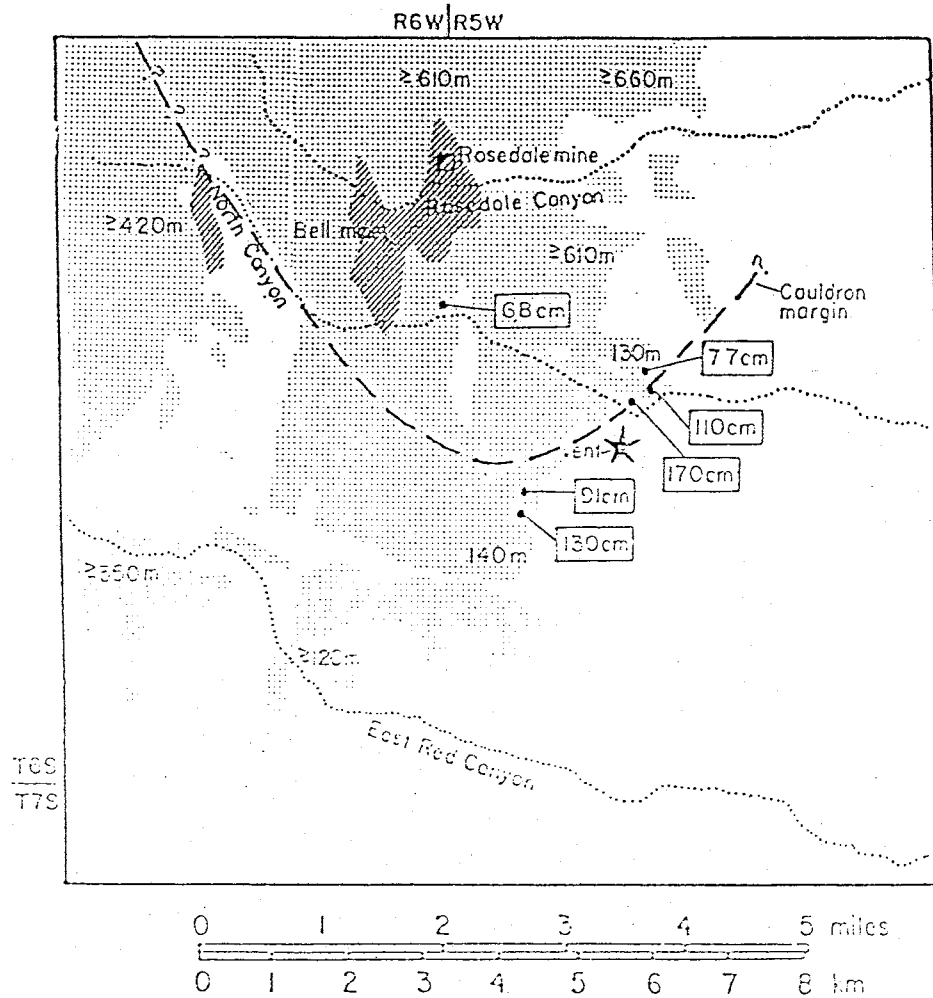
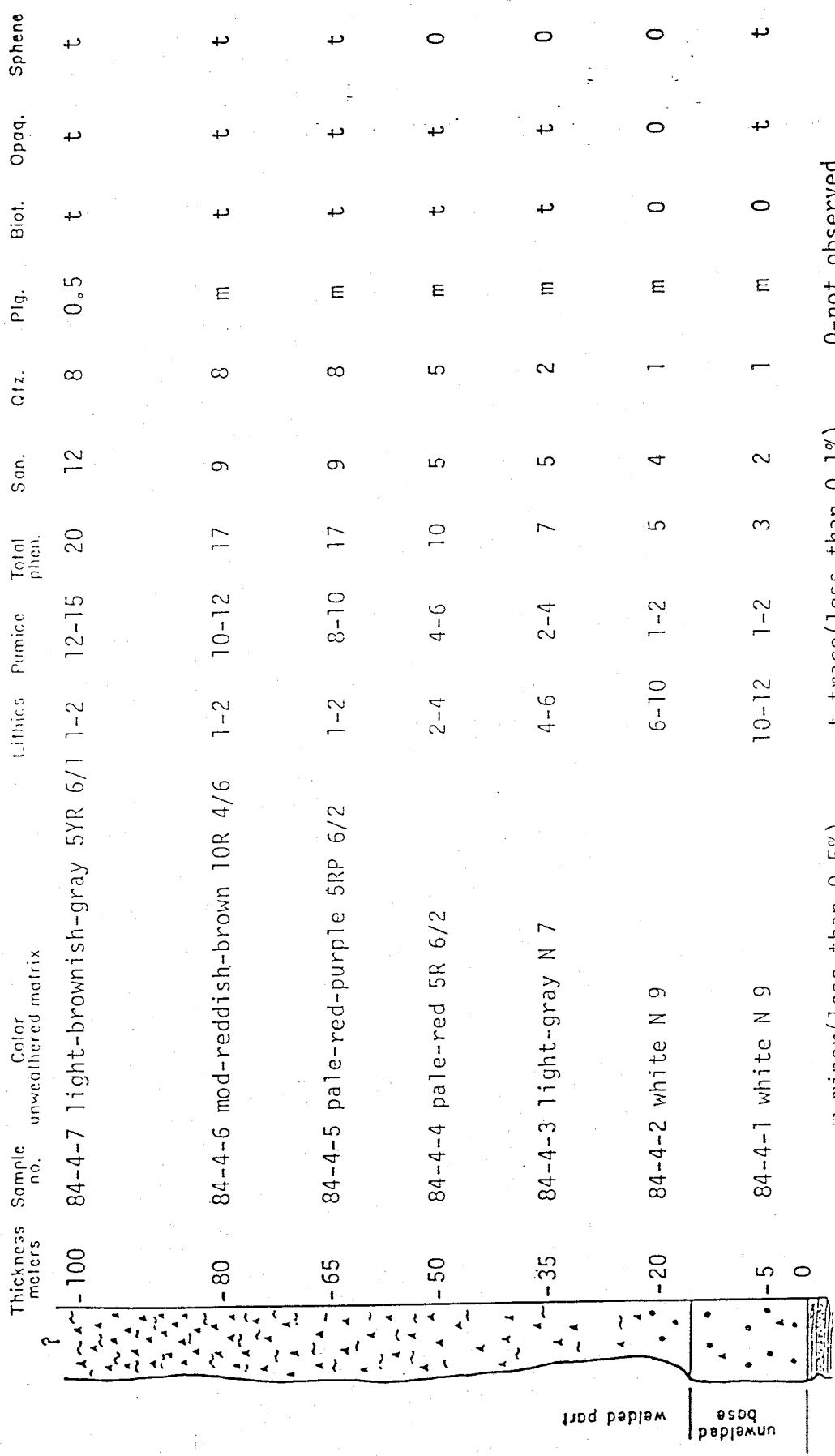


Figure 25. Outcrop map of the South Canyon Tuff showing the average size of the five largest lithic fragments (in centimeters) in exposures of lithic breccias in the unit. Also shown are thicknesses of the unit (meters), zones of hydrothermal argillic alteration (lined pattern), and a possible vent area for the South Canyon Tuff.

Figure 26, and for the other samples in Table 2. The unit is vertically zoned with phenocryst percentages increasing from 2% at the base to 35% at the top. The vertical increase is gradual up to about 25%, but the increase from 25% to 35%, which is only observed in the north, is rapid, and occurs in the upper 20-30m of the unit.

In most thin sections of the South Canyon Tuff the matrix, which is only partially devitrified, contains well preserved glass shards. Undeformed glass shards (0.1-0.5mm long) are found at the base, but in the lineated part, shards are stretched up to 1.0mm long, and have compaction ratios >20:1.

Phenocrysts in the South Canyon Tuff consist mostly of sanidine and quartz in an approximate 3:2 ratio, with minor amounts of plagioclase and biotite, and trace amounts of opaque minerals, and sphene. Sanidine occurs as blocky euhedral grains (1-3mm), and quartz as blocky subhedral grains (1-3mm) that are usually resorbed. Plagioclase, which rarely composes more than 2% of the tuff, occurs either as individual subhedral grains (<1mm) or in glomeroporphyritic growths (1-3mm) with biotite, sphene, or opaque minerals. Biotite occurs as flakes (0.5-1.0mm), and opaque minerals as rounded grains (<0.5mm). Sphene occurs as euhedral grains up to 1.5mm long, but which average 0.5mm.



m-minor (less than 0.5%) t-trace (less than 0.1%) 0-not observed

Figure 26. Stratigraphic section of the South Canyon Tuff measured at Turkey Spring (sec. 35, T6S, R6W). Visual estimates of phenocryst percentages are from thin sections, and lithic and pumice percentages are estimated from hand specimens.

- ~ Pumice fragments
- Lithic fragments
- ▲▲ Phenocrysts

Table 2. Petrographic data from samples of the South Canyon Tuff (not including data from Figure 26.) throughout the study area. Phenocryst percentages are visually estimated from thin sections, and lithic and pumice percentatges are estimated from hand specimens.

Sample no.	Lithics	Pumice	Total phen.	Son.	Qtz.	Plg.	Biot.	Opaq.	Sphene
83-41	2	-	2	1	1	-	-	-	t
83-47	10	-	6	3	3	-	-	-	-
83-145	3	7	6	3	3	m	t	t	-
83-129	3	10	7	3	3	1	t	t	-
83-103	3	15	9	4	5	m	m	t	-
83-102	2	10	12	6	5	0.5	t	t	t
83-181	4	10	12	6	6	-	t	t	t
83-99	3	15	15	7	7	1	t	t	-
83-128	2	17	15	10	5	m	t	t	t
83-104	7	5	15	7	5	2	t	t	t
83-151	5	15	17	10	6	1	t	t	-
83-118	t	10	20	12	6	2	m	m	t
83-153	5	12	20	9	10	0.5	m	t	t
83-152	5	15	23	12	10	-	m	m	t
83-125	1	12	25	15	9	m	m	m	t
84-168	5	10	35	20	13	1.5	0.5	m	t

m=minor(less than 0.5%)

t=trace(less than 0.1%)

-not observed

Pumice fragments less than 5mm long compose <1% of the basal South Canyon Tuff at the Turkey Spring section. Pumice gradually increase in size (2-3cm) and in abundance (up to 5%) from 0-50m above the base. From 50-60m pumice content increases rapidly to 10%. Above 60m, the unit contains 12% to 15% pumice fragments that average 5-10cm in length. Most of the pumice fragments in the South Canyon Tuff are completely replaced by vapor-phase intergrowths of sanidine and quartz. In the center of some of the largest fragments there is an interstitial growth (<0.2mm) of a highly birefringent mineral. This mineral, which appears to be the last phase to crystallize in the pumice, may be an incompatible-element-enriched mineral such as allanite.

In the south, South Canyon Tuff pumice fragment compaction ratios are usually less than 10:1. In the north, where the base of the unit is a black to dark-reddish-brown vitrophyre 5-15m thick, pumice fragments may be 20cm long, and have length to thickness ratios greater than 20:1. Much of the pumice in the north is elongated and preferentially oriented (Fig. 27). In the northwest part of the study area, pumice fragments are usually oriented only in tuff with phenocryst contents between 3% and 12%. However, in the north and northeast, pumice fragments are usually more elongated, and they are aligned in tuff with phenocryst contents as high as 25%. Field azimuth measurements of these aligned pumice fragments are plotted in Figure 28.

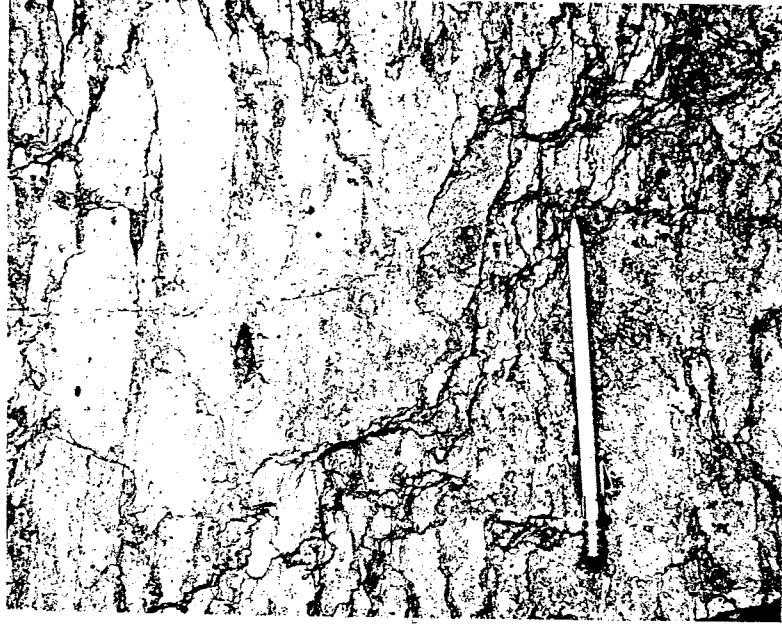


Figure 27. Photograph of lineated pumice in the South Canyon Tuff (sec. 10, T6S, R6W).

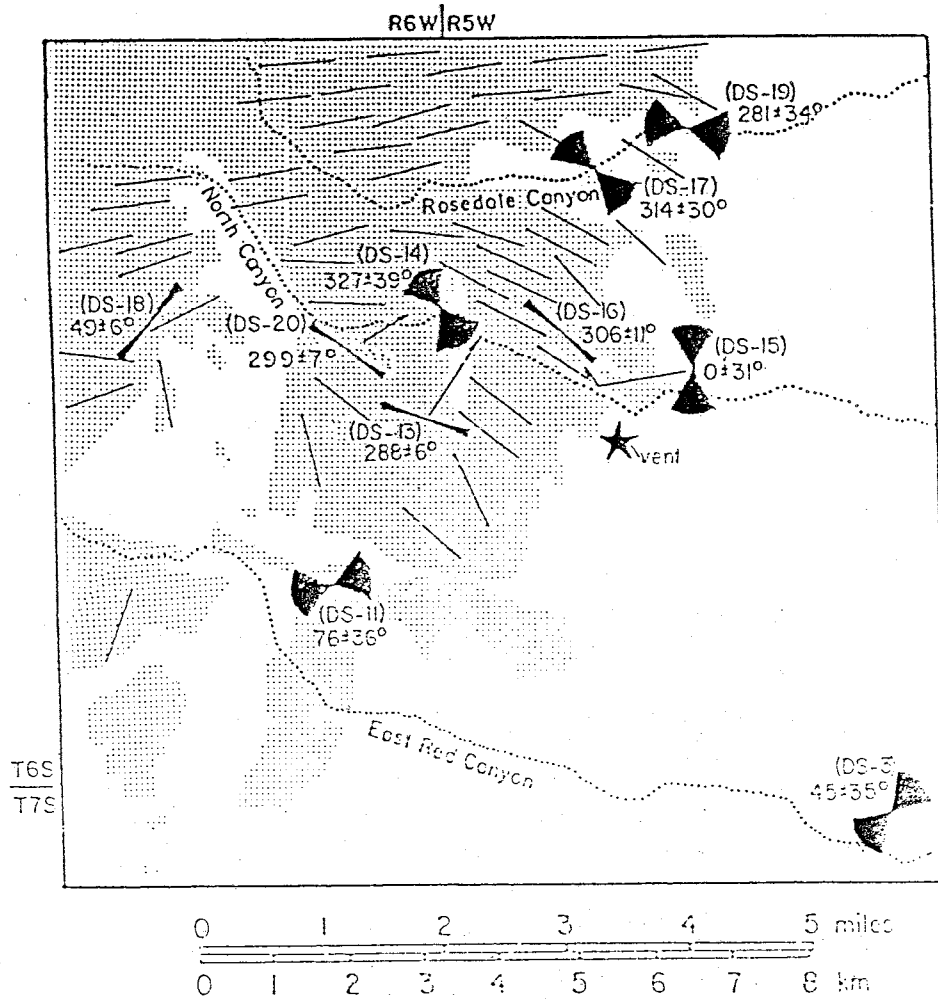


Figure 28. Outcrop map of the South Canyon Tuff showing field measurements of lineated pumice and magnetic anisotropy of susceptibility azimuth cones of confidence (95% level). Paleomagnetic sample numbers are shown with each anisotropy azimuth. A possible vent area for the South Canyon Tuff is also shown.

The base of the South Canyon Tuff, at the Turkey Spring section, contains 10-15% lithic fragments (0.2-2.0cm) consisting of rhyolite and basaltic andesite lava. Lithic content decreases upward to less than 1% 50m above the base. The upper part of the unit, in the south, contains only minor amounts of lithics, but in the north it contains swarms of lithics within welded matrix-supported tuff. Lithic fragments (consisting mostly of rhyolite lava and Lemitar Tuff) in these swarms rarely exceed 20cm in diameter, and typically compose less than 30% of the tuff. These swarms may be distal equivalents of the clast-supported lithic breccias member exposed near Wildcat Peak. Clasts of medium to fine-grained biotite-rich monzogranite (IUGS classification) are minor, but significant contributors to the population of lithic fragments in the uppermost South Canyon Tuff.

Hydrothermal alteration

In the north part of the study area, the South Canyon Tuff hosts two abandoned epithermal gold mines (Rosedale Mine, Bell Mine). At these mines, according to Neubert (1983), mineralized veins parallel basin and range faults that trend 340 degrees and dip about 75 degrees to the west. Argillic alteration, associated with the mineralization, is concentrated along faults throughout the area, and along the Lemitar-South Canyon contact on the west side of North

Canyon. Mineralization in the area was not investigated in detail, but zones of alteration are roughly outlined in Figure 25.

Units younger than the South Canyon Tuff

There are three units in this study area younger than the South Canyon Tuff, all restricted to the northern part of the study area. In the north-central part of the area, the South Canyon Tuff is overlain by the unit of North Canyon, and is intruded by the rhyolite lava dome of Wildcat Peak. In the northeast corner of the study area, the South Canyon Tuff is overlain by the tuff of Rosedale Canyon.

Unit of North Canyon

The unit of North Canyon's top is not exposed, but it is at least 50m thick about 2km north of Wildcat Peak. Here it fills a slight depression that is, north to south, about 1km across. The unit's lower contact is a slight angular unconformity.

The unit of North Canyon consists mostly of epiclastic rocks (diamictite, conglomerate, and cross-stratified sandstone), but also contains lithic-rich poorly welded ash-flow tuffs (<2m thick), and pyroclastic breccias. Pyroclastic rocks of the unit are spatially related to the rhyolite dome of Wildcat Peak, and are probably derivatives

of it. Epiclastic rocks in the unit, derived partly from erosion of these pyroclastic rocks, become finer grained, and more voluminous to the north and west. Cross-stratified sandstones in the unit, similar to those in the unit of East Red Canyon, are also interpreted as eolian. Clasts in all lithologies of the unit consist mostly of crystal-rich tuff, and rhyolite lava, but minor amounts of granite are also present.

Intrusive rhyolite of Wildcat Peak

The intrusive rhyolite of Wildcat Peak is named for a resistant plug (it's principle source) that intrudes the South Canyon Tuff at the intersection of Exter Canyon and North Canyon in the east central part of the study area. The rhyolite is also found to the north as a series of east-northeast trending dikes (Plate 1).

In thin section (85-7) the rhyolite of Wildcat Peak contains phenocrysts of sanidine (3%), and plagioclase (3%). Trace amounts of biotite, sphene, amphibole, and opaque minerals are also present. Sanidine and plagioclase occur as blocky euhedral crystals (2mm). Quartz is present only as a vapor phase mineral in lithophysae cavities.

Tuff of Rosedale Canyon

The tuff of Rosedale Canyon is a moderately crystal-rich rhyolite ash-flow tuff that overlies the South Canyon Tuff in the extreme northeast corner of the study area. In this study area the base of the unit is not exposed, and poor exposure makes it impossible to describe a vertical section. However, a sample collected from near its base was studied in thin section (84-167). This sample contains about 15% phenocrysts of euhedral blocky sanidine (0.5-2.0mm), and blocky euhedral resorbed quartz (0.5-2.0mm) in an approximate 2:1 ratio. Blocky subhedral plagioclase (0.5mm) occurs in minor amounts. Biotite (0.5mm), euhedral sphene (0.5mm), and opaque minerals (0.3mm) occur in trace amounts. The matrix of the tuff is completely devitrified (no evidence of shards), and contains spherical lithophysae (2mm) filled with vapor phase sanidine and quartz. Pumice fragments (about 1cm long), replaced by vapor phase quartz and sanidine, compose about 3% of the tuff. Although densely welded (compaction ratios of 10:1), there is no apparent elongation or preferred orientation of the pumice fragments. Lithic fragments of South Canyon Tuff and basaltic andesite (2mm-2cm) compose about 3-5% of the tuff.

CHAPTER 3
STRATIGRAPHY

Introduction

Figure 29 illustrates the stratigraphic sequence for this study area, and compares it with the regional stratigraphy for the northeast Datil-Mogollon volcanic field (Osburn and Chapin, 1983). Figure 29 also includes high precision $^{40}\text{Ar}/^{39}\text{Ar}$ dates of the 5 regional ash-flow tuffs (Kedzie and others, 1985). All rocks exposed in the study area are Oligocene and possibly Miocene silicic volcanic and volcanoclastic rocks. The oldest regional unit is the Oligocene La Jencia Tuff (28.8 Ma), and the youngest is the South Canyon Tuff (27.4 Ma).

The stratigraphic sequence is not exposed continuously anywhere in the study area. The lower part of the sequence consists of outflow sheets of regional ash-flow tuffs that are exposed mostly in the southeast corner of the study area. To the west, the lower part of the sequence is downfaulted and buried by younger rocks. These younger rocks, not preserved in the southeast part of the study area, consist of local tuffs, lavas, volcanoclastic sediments, and a >600m thick sequence of the South Canyon Tuff.

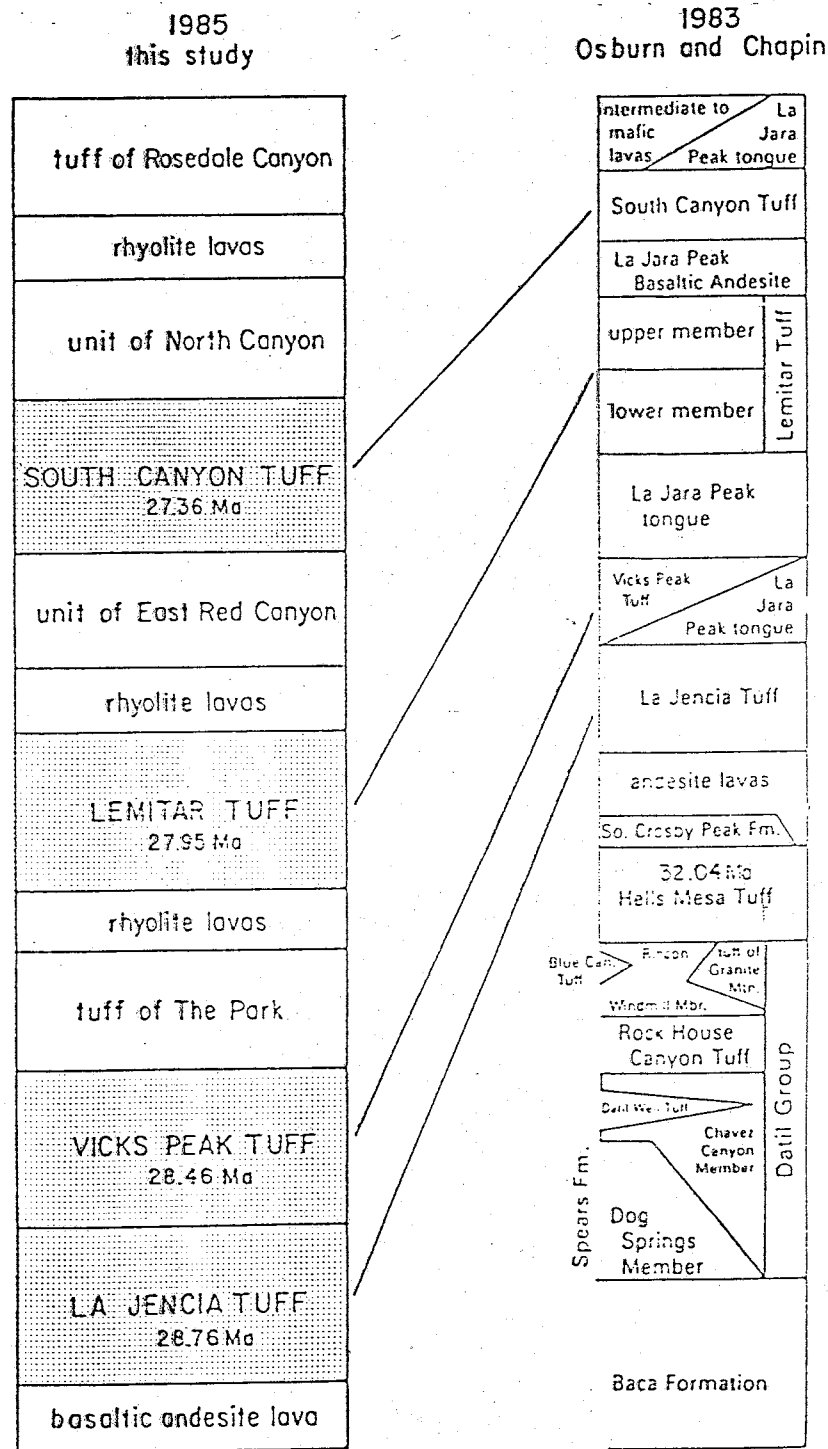


Figure 29. Stratigraphic sequence from this study compared with the regional stratigraphy of Osburn and Chapin (1983). Also shown are high precision $^{40}\text{Ar}/^{39}\text{Ar}$ dates (± 0.15 m.y.) of the regional ash-flow tuff units (Kedzie and others, 1985). The regional ash-flow tuffs are shown with a stippled pattern.

The stratigraphic sequence is intruded, throughout the study area, by at least three generations of crystal-poor rhyolites.

Correlation with previous work

Figure 30 correlates the stratigraphic sequence from this study area with stratigraphic sequences for adjacent areas described by Deal (1973), Donze (1980), and Atwood (1982).

Comparing Deal's (1973) stratigraphy with this study's detailed stratigraphy (Fig. 30) reveals several inconsistencies with his stratigraphic interpretation. The tuff mapped by Deal (1973) as the Hells Mesa Tuff was correlated with the Lemitar Tuff in this study for three reasons: 1) it's stratigraphic position below the South Canyon Tuff; 2) it's distinctive quartz-poor interval; and 3) it's normal paleomagnetic polarization (Hells Mesa Tuff is reverse polarized; McIntosh, 1983). In the northern part of the study area, Deal's (1973) A-L Peak Tuff was correlated with the South Canyon Tuff, because it overlies the Lemitar Tuff, and contains subequal amounts of quartz and sanidine phenocrysts. In the south Deal's (1973) A-L Peak Tuff was correlated with the La Jenica Tuff, because it underlies the Lemitar Tuff, and contains only sanidine phenocrysts. The Potato Canyon Tuff, mapped by Deal (1973),

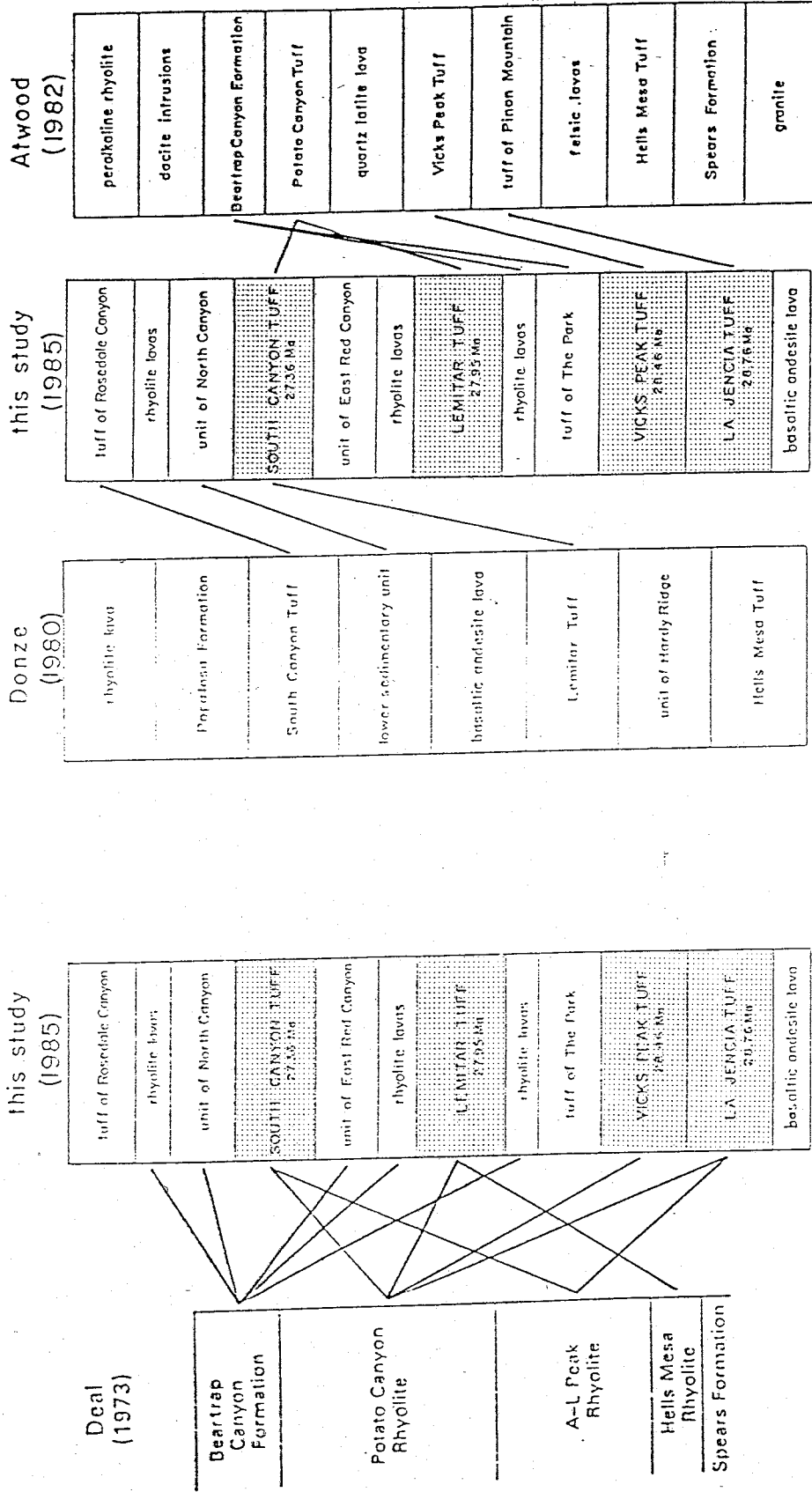


Figure 30. Stratigraphic sequence from this study (regional ash-flow units shown with a stippled pattern) compared with the stratigraphic sequences of previous workers in adjacent areas (see Fig. 1).

was correlated with the South Canyon Tuff in the northern part of this study area, and in the south, it was correlated with 4 regional regional ash-flow tuff sheets. These outflow sheets (La Jencia, Vicks Peak, Lemitar, and South Canyon Tuffs) are separated by major cooling breaks, and are distinguished by individually distinct petrographic and paleomagnetic properties. Deal's Beartrap Canyon Formation (moat deposits) consists of all felsic lavas and sedimentary rocks in the study area, regardless of their age. This study recognizes 3 sequences of felsic lavas, and 2 sequences of sedimentary rocks. Deal (1973) approximately located the southeast margin of a cauldron in this study area. However, the use of an oversimplified stratigraphy prevented him from recognizing the complexity of the structure.

The lower part of Atwood's (1982) stratigraphic sequence (below the Vicks Peak Tuff) correlates well with that established in this study area (Fig. 30). Overlying the Vicks Peak Tuff, to the south of this study area, are a variety of felsic lavas, tuffs, and volcanoclastic sediments which were grouped by Atwood (1982) into the Beartrap Canyon Formation. A 300m thick sequence of these rocks overlies the Vicks Peak Tuff to the west of a major west-side down fault in the western part of Atwood's area. Atwood, however, places the Beartrap Canyon Formation above his Potato Canyon Tuff, even though he has no direct evidence for this

relationship. Atwood further uses the Potato Canyon Tuff to include all major ash-flow tuffs younger than the Vicks Peak Tuff (Osburn, personal communication). This lumping makes it impossible to compare mapping of the younger units (particularly in the northern part of his area) with mapping in this study area.

Rocks in the upper part of Donze's (1980) stratigraphic sequence were named before the regional stratigraphy of Osburn and Chapin (1983) was established, but otherwise correlate well with the upper part of the stratigraphic sequence in this study area (Fig. 30). In the eastern part of Donze's (1980) map area, the tuff mapped as the Lemitar Tuff is actually the South Canyon Tuff, and the South Canyon Tuff is a younger local ash-flow tuff that may correlate with the tuff of Rosedale Canyon of this study (Fig. 30). Between these two tuff units Donze mapped a sequence of volcanoclastic sediments that is correlated with the unit of North Canyon in this study area.

The miscorrelated A-L Peak Tuff, and the Potato Canyon Tuff (combined unit) have been abandoned by Osburn and Chapin (1983) in favor of more specific unit names. The Beartrap Canyon Formation has been used for sedimentary rocks, and associated "moat deposits" related to at least two different cauldrons in the San Mateo Mountains (Deal, 1973; Deal and Rhodes, 1976; Atwood, 1982). Therefore, to

avoid confusion in this study area, all local lavas, tuffs, and sedimentary rocks are given individual informal names until stratigraphic relations are better understood.

Stratigraphy of this study area

Introduction

Each stratigraphic unit in this study area is described in detail in Chapter 2. This section summarizes the important stratigraphic relationships. The Lemitar Tuff is a useful marker horizon with which to compare lateral changes in stratigraphy, because it is the only unit that can be positively identified throughout the study area. In the southeast part of the study area, the Lemitar Tuff overlies outflow sheets of the La Jencia and Vicks Peak Tuffs. In the western part, however, the Lemitar overlies different rocks which are thought to be younger than the Vicks Peak Tuff.

Units older than the Lemitar Tuff

LA JENCIA TUFF

The La Jencia Tuff, at least 270m thick in this study area, is a crystal-poor sanidine-bearing rhyolite ash-flow tuff. It is strongly flow-banded with a consistent

east-west lineation (Fig. 5). The base is exposed only in the eastern part of North Canyon where it overlies at least 60m of basaltic andesite lava (Plate 1).

VICKS PEAK TUFF

The Vicks Peak Tuff is a crystal-poor sanidine-bearing rhyolite ash-flow tuff that is flow-banded and lineated only in the southern part of the study area. Pumice fragments here are consistently oriented northwest-southeast. The unit, which conformably overlies the La Jencia Tuff, thickens from <100m to >300m to the southwest (Fig. 7) where it's base is not exposed.

TUFF OF THE PARK

In the western part of the study area, the La Jencia and Vicks Peak Tuffs are not exposed. Instead, the Lemitar Tuff overlies the tuff of The Park which is a moderately welded crystal-rich quartz, sanidine-bearing rhyolite ash-flow tuff whose outcrop area is shown in Figure 9. The author assumes that the tuff of The Park is younger than the Vicks Peak Tuff even though there is no established age relationship between the two anywhere in the study area. This interpretation is compatible with mapping by Atwood (1982) to the south of here, which shows Vicks Peak Tuff buried by local tuffs and lavas (Beartrap Canyon Formation)

to the west of a major west-side down fault. The local tuffs and lavas in Atwood's area (exposed only to the west of the fault) are correlated in a general sense with the tuff of The Park, and pre-Lemitar intrusive rhyolites in this study area (Fig. 30).

Lemitar Tuff

The Lemitar Tuff is a crystal-poor to crystal-rich quartz, sanidine, plagioclase-bearing rhyolite ash-flow tuff. It is only 5-15m thick in the southwest part of the study area, but it thickens to 80m to the north, and about 240m to the east. The Lemitar Tuff also fills north and northeast trending paleocanyons, cut into the Vicks Peak Tuff, in the eastern half of the study area. These lateral variations in thickness, and the trend of paleocanyon walls (Fig. 12) suggest that the southwest corner of the study area was a highland before deposition of the Lemitar Tuff.

Unit of East Red Canyon

The unit of East Red Canyon is a sequence of volcanoclastic conglomerates, sandstones, and minor pyroclastic rocks which fills a post-Lemitar, pre-South Canyon structural basin (200m deep) in the southwest corner of the study area. The minimum volume of material in the basin, including a partially buried rhyolite dome, is about

5km³. The eastern part of the basin was filled by an alluvial fan complex derived from erosion of the basin's eastern structural margin. Alluvial fan deposits grade westward into a sequence of eolian sandstone transported from the southwest.

South Canyon Tuff

The South Canyon Tuff is a crystal-poor to crystal-rich quartz, sanidine bearing rhyolite ash-flow tuff. It fills a structural basin in the north-central part of the study area where it is at least 600m thick. Parts of the unit are strongly flow-banded with lineations in the northern part of the study area oriented about N80E. To the south, towards the southeast margin of the basin, lineations swing around to N50W (perpendicular to the margin) and the tuff thins to <150m (Fig. 28). Southeast of this margin, it is not known how thick the South Canyon Tuff is, or even if it was ever deposited. A few thin exposures of unwelded tuff there are tentatively correlated with the base of the South Canyon Tuff (Plate 1; Fig. 28).

Along the basin's southeast structural margin, lenses of clast-supported lithic breccia are distributed vertically and laterally throughout the South Canyon Tuff (Plate 1). The average size of lithic fragments in the breccias (Fig. 25) decreases from 170cm to 70cm away from the margin. The

breccias are similar to co-ignimbrite lag-fall deposits, defined by Wright and Walker (1977) as accumulations of lithic fragments too large to be carried away from the impact area of a collapsing eruption column. The breccias in this area are thought to have been deposited by a collapsing eruption column from a nearby vent or vents. The rhyolite dome of Wildcat Peak, located along the basin's southeast margin, is thought to intrude and seal a vent for the South Canyon Tuff, and the basin is interpreted to be the south end of the South Canyon Tuff's cauldron.

Intrusive rhyolites

There are at least three generations of intrusive crystal-poor rhyolite in the study area (Plate 1). The first generation, older than the Lemitar Tuff and younger than the Vicks Peak Tuff or tuff of The Park, was intruded along the northwest margin of a post-Vicks Peak Tuff depression in the southern part of the study area. The second generation includes post-Lemitar, pre-South Canyon intrusive rhyolites that were intruded along the southeast structural margin of the unit of East Red Canyon's basin and the South Canyon Tuff's cauldron. The third generation of rhyolites (younger than the South Canyon Tuff) intruded the southeast structural margin of the South Canyon Tuff's cauldron. There are many rhyolites in the study area whose

exact age is poorly constrained (Plate 1). These rocks are tentatively correlated with the second generation of rhyolites because they contain quartz and feldspar phenocrysts, and the others contain only feldspar (Chapter 2).

Summary

The stratigraphic nomenclature used by Deal (1973) for the northern San Mateo Mountains was found to be inadequate for the detailed mapping in this study area. Stratigraphic nomenclature described by Osburn and Chapin (1983) for the Socorro region was used for regional units exposed in this study area.

The oldest units in the study area consist principally of outflow sheets of the La Jencia, Vicks Peak, and Lemitar Tuffs which crop out in the southeast corner. To the west, the Vicks Peak Tuff is buried by local volcanic units that are thought to fill a depression related to the Vicks Peak's eruption. Following subsidence, this area was uplifted and dissected by north and northeast directed canyons which were subsequently filled with Lemitar Tuff.

Outflow sheets of the La Jencia, Vicks Peak, and Lemitar Tuffs in the southeast part of the study area are largely truncated to the west by a post-Lemitar structural basin. This basin filled with at least 200m of

volcaniclastic conglomerate and eolian sandstone in the south, followed by deposition of at least 600m of South Canyon Tuff to the north. A vent for the South Canyon Tuff, intruded by a younger rhyolite dome, is located along the basin's southeast structural margin. The basin to the north is thought to be the south end of the South Canyon's cauldron.

CHAPTER 4

STRUCTURE

Introduction

There are two types of structures in this study area, early syn-volcanic depressions and later extension related normal faults. The oldest structures are two major syn-volcanic depressions, one in the south filled with Vicks Peak Tuff, and one in the north filled with South Canyon Tuff. These syn-volcanic structures are cut by north-south (down to the west) faults throughout the study area, and east-west (down to the south) faults in the southern half of the study area. The younger faults are the result of Basin and Range extension (Chapin, 1979), which has tilted fault blocks to the east throughout the study area. Dips increase gradually from 5-15 degrees in the south to 30-50 degrees in the north.

Volcanic Structures

Structures related to the Vicks Peak Tuff

The oldest volcanic structure in the study area is a proposed depression in the southwest corner filled with Vicks Peak Tuff (Fig. 31). Since this part of the study

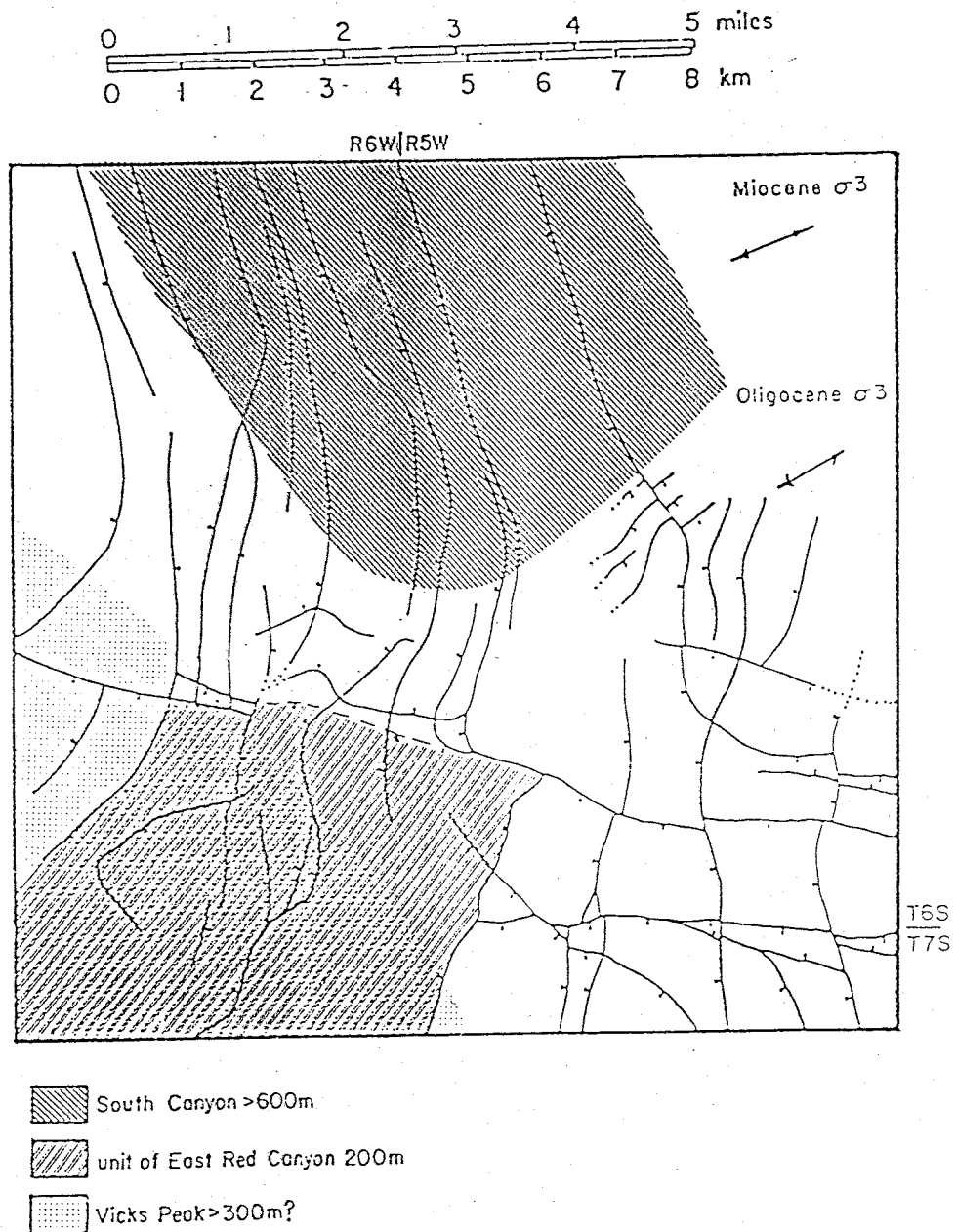


Figure 31. Structural map of the study area showing the extent of structural depressions filled by the Vicks Peak Tuff, the unit of East Red Canyon, and the South Canyon Tuff. Also shown are approximate thicknesses of each unit within it's depression. The Miocene $\sigma 3$ is from Zoback and others (1981), and the Oligocene $\sigma 3$ is from this study (see Table 3).

area is mostly buried by deposits related to a younger structure, all evidence for this subsidence is stratigraphic. The stratigraphic evidence is essentially southwestward thickening of the Vicks Peak Tuff, and burial of the Vicks Peak Tuff by local volcanic units. The eastern edge of the depression, illustrated in Figure 31, is a continuation of a west-side down fault in Atwood's area (1982), across which the Vicks Peak Tuff is buried by local volcanic units. Uplift in the southwest, after deposition of the local volcanic units, is indicated by southwest thinning of the Lemitar Tuff, and is evidence for post-Vicks Peak cauldron resurgence.

Structures related to the South Canyon Tuff

SOUTH CANYON TUFF CAULDRON MARGIN

In the northern part of the study area, the South Canyon Tuff (at least 600m thick) occupies a structural depression (Fig. 31) whose bottom is not exposed. The depression is thought to be part of the South Canyon Tuff's cauldron, largely because of the syn-volcanic nature of its southeast margin. This margin, best exposed near Wildcat Peak, is a northeast trending monoclinial structural zone that is at least 2km wide. The structural zone consists of northwest tilted pre-South Canyon strata (25-60 degrees). These strata are repeated by closely spaced east-side down

faults which dip normal to the truncated units (Plates 1,2,3). On the east edge of the zone, the transition from untilted to tilted strata occurs abruptly across a narrow (<20m wide) fault zone. The western edge of the structure is buried by welded South Canyon Tuff. The youngest rocks affected by this structure are bedded tuffs of the upper unit of East Red Canyon and a basal clast-supported lithic breccia of the South Canyon Tuff. The age of the structure is therefore constrained to be during the eruption of the South Canyon Tuff. The intrusive rhyolite of Wildcat Peak (Plate 1) is undeformed by faults related to the structure, and is thought to seal a vent for the South Canyon Tuff. A series of rhyolite dikes, trending about N55E, intrude the South Canyon Tuff to the north of the margin (Plate 1). This suggests that, in this area, a localized least principle stress field was oriented about N35W during intrusion of the dikes.

A model for the development of this structural zone is illustrated in Figure 32. The model depicts a flat topped magma chamber, at a depth of about 2-3km, feeding dikes along it's southeast margin. A major pyroclastic eruption occurs using these dikes as conduits. Subsequent magma evacuation causes collapse of the cauldron block, and downsagging along the margin. After the eruption, devolitalized magma (intrusive rhyolite of Wildcat Peak) seals the pyroclastic vent(s).

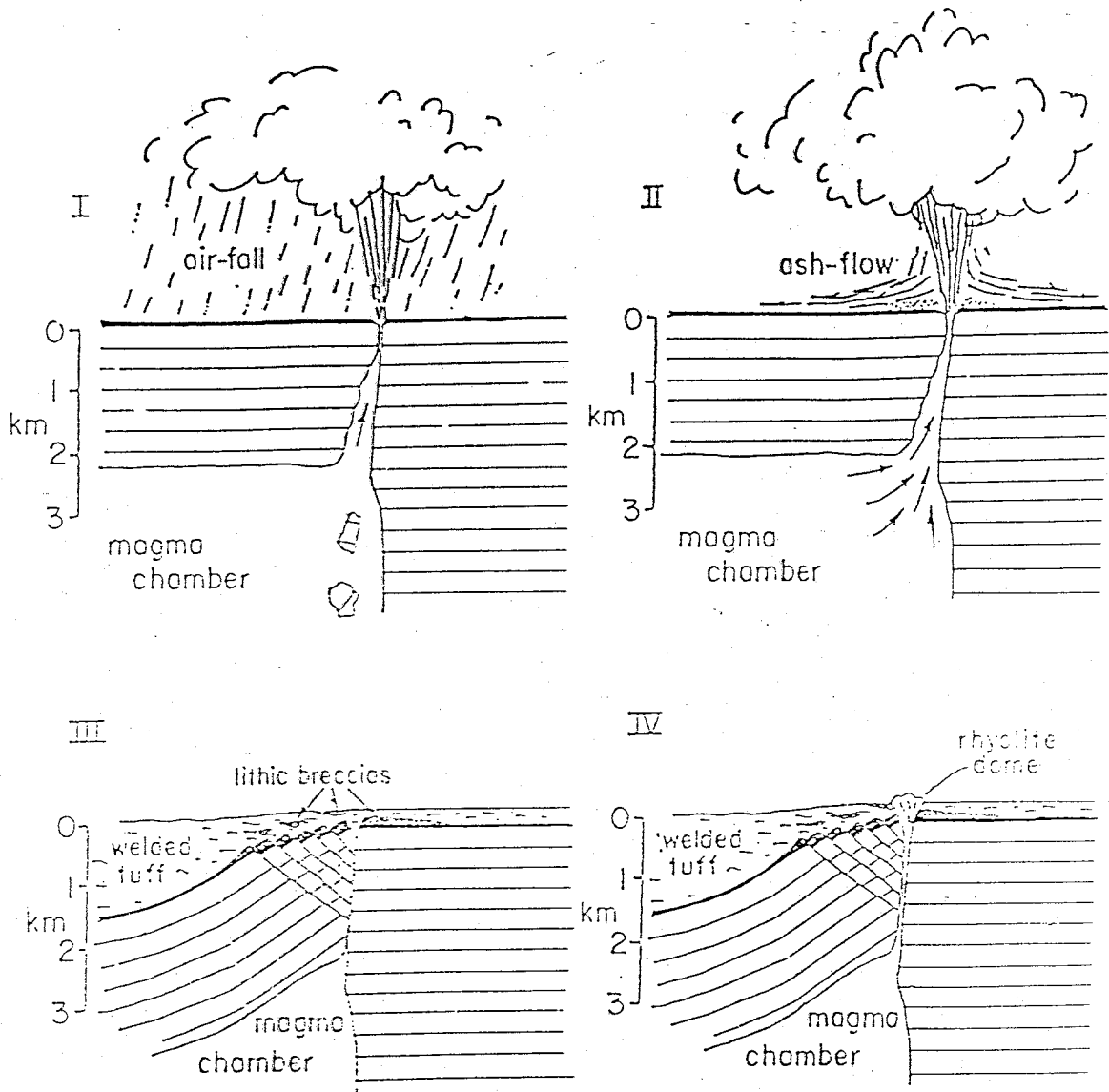


Figure 32. Four stage model for the formation of the southeast structural margin of the South Canyon Tuff's cauldron, see text for discussion.

The western margin of the South Canyon cauldron in this study area is thought to coincide with an east-side down fault in North Canyon (Fig. 31). The margin is placed here because the South Canyon Tuff's base is exposed to the west of the fault, but not to the east. To the south, the cauldron margin is extended to include area where the South Canyon's base is not exposed.

SEDIMENTARY BASIN OF THE UNIT OF EAST RED CANYON

The unit of East Red Canyon fills a northeast trending basin in the southwest corner of the study area. The basin subsided after deposition of the Lemitar Tuff and was eventually covered by the South Canyon Tuff. The basin extends to the south of a 1-2km wide east-west structural horst (Plate 3) that separates it from the South Canyon cauldron. The structural style that characterizes the southeast margin of the South Canyon cauldron is thought to continue south, and compose the eastern structural margin of the sedimentary basin. Evidence for this structure, however, is mostly buried by basin filling sediments (Plate 1,3). The western margin of the basin is a northeast trending east-side down fault (Plate 1).

The northern extent of the sedimentary basin is poorly constrained, but it is thought to terminate against a south-side down fault which extends across the lower third of the study area (Fig. 31). Along the northern edge of the basin, the fault (dashed on Fig. 31) is buried by the South Canyon Tuff. Basin sediments are thought to thin abruptly across the fault to the north (Plate 3). The main line of evidence for this thinning is an abrupt southward decrease in the density of welding of the overlying South Canyon Tuff. In the south, the South Canyon has a thick (30-70m) unwelded base, but to the north, the base is a vitrophyre, and the tuff is strongly lineated. The difference in welding is attributed to the cooler, perhaps water saturated, underlying sediment to the south, compared to the underlying volcanic rocks to the north. The thickness of the unwelded base in the south decreases northward stepwise across faults which do not cut the overlying welded tuff (Plate 3). These faults were probably activated during eruption of the tuff, and may be related to the proposed northern termination of the basin (Plate 3).

Basin and Range structures

FAULT PATTERNS AND THE LEAST PRINCIPLE STRESS FIELD

Rocks in the study area were broken into both north-south trending and east-west trending fault blocks as a result of Basin and Range extension which was initiated about 32-27 Ma (Chapin, 1979). From south to north, faults change from an orthogonal north-south and east-west pattern to a northwest-southeast parallel pattern (Fig. 33). The change in fault patterns is thought to reflect the control of different basement structures on a late Oligocene to Miocene N63E to N70E regional least principle stress field. The late Oligocene regional least principle stress direction (N63E) was determined from the trends of rhyolite dikes in this study area (Table 3). The Miocene direction (N70E) is an average of two directions from a compilation by Zoback and others (1981, p. 423). The resultant vector of Basin and Range extension for any part of the study area, regardless of how different the fault patterns are, is generally parallel to this least principle stress field.

In the south, the orthogonal fault pattern is probably controlled by pre-Tertiary basement fractures. As faults cross the proposed South Canyon cauldron margin, from south to north, they curve sharply to the northwest. Within the cauldron, faults appear to be controlled only by the least

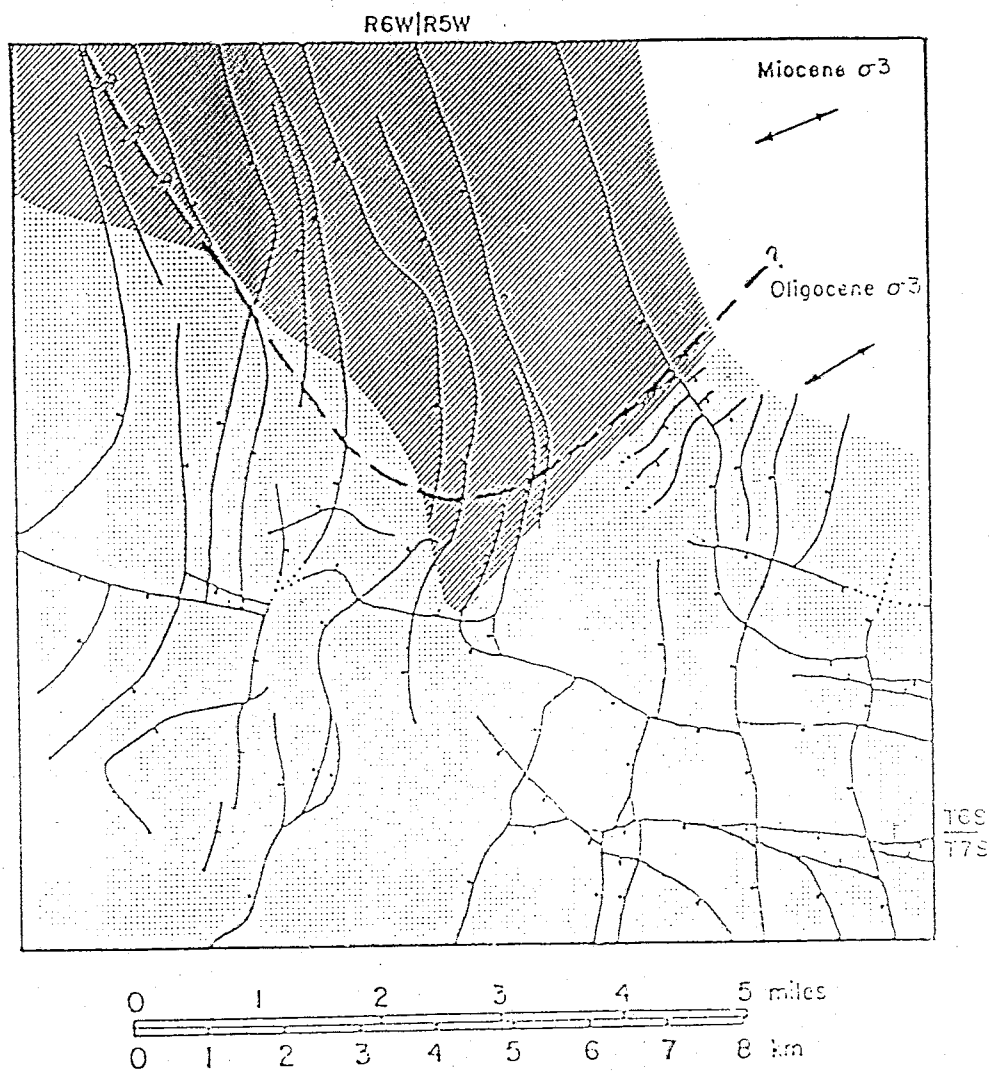


Figure 33. Structural map of the study area showing the moderately extended domain (lined pattern), and the weakly extended domain (stippled). Also shown is the proposed South Canyon Tuff cauldron margin (dashed heavy line). The Miocene $\sigma 3$ is from Zoback and others (1981), and the Oligocene $\sigma 3$ is from this study (see Table 3).

Table 3. The location and age constraints of dikes in the study area whose trends are thought to have been determined by a regional stress field.

trend of dike	least principle stress direction	location	name of intrusive	age constraints
N30W N26W	N60E N64E	N1/2 sec. 28, T6S, R5W } S1/2 sec. 28, T6S, R5W }	rhyolite of Horse Mountain	post-Lemitar (28.0 Ma) pre-?
N24W N27W	N66E N63E	N1/2 sec. 5, T7S, R5W } W1/2 sec. 5, T7S, R5W }	rhyolite of Drift Fence Canyon	post-Vicks Peak (28.5 Ma) pre-Lemitar (28.0 Ma)

principle stress field. The author suggests that a shallow pluton beneath the South Canyon cauldron (Fig. 32) negated the effect of older basement fractures on the fault patterns here.

MAGNITUDE OF TILTING AND THE AGE OF BASIN AND RANGE EXTENSION

Apart from a northeast trending zone of west-tilted rocks related to the margin of the South Canyon Tuff's cauldron, all rocks in the study area are tilted to the east from 5-50 degrees. The tilting increases gradually from 5-15 degrees in the south to 30-50 degrees in the northern part of the study area.

In a study of Tertiary tectonics of the Socorro region, Chamberlin and Osburn (1984) relate the degree of tilting to the amount of Basin and Range extension that has occurred. They define domains of weak (0-30%), moderate (30-100%), and severe (100-200%) extension by low (1-20 degrees), intermediate (20-50 degrees) and steep (50-70 degrees) dips, respectively, of Oligocene strata. This study area is divided into the weakly extended domain in the south, and the moderately extended domain in the north, with the boundary coinciding approximately with the proposed margin of the South Canyon cauldron (Fig. 33).

Before deposition of the unit of North Canyon, in the northern part of the study area, older rocks (South Canyon Tuff) had been tilted east about 10 degrees. Deal (1973) interpreted this tilting as evidence for resurgence of his Mt. Withington cauldron. It is also possible that the unit of North Canyon was deposited after Basin and Range extension had tilted older units 10 degrees to the east. Basin and Range extension was probably initiated by at least the time of the eruption of the South Canyon Tuff (27.4 Ma). The duration of extension is constrained only by Quaternary pediment gravels which are undeformed by faults, throughout the study area. From stratigraphic and geomorphic evidence in the Socorro area, Chamberlin and Osburn (1984) suggest that the weakly extended domain was stretched from 31 Ma to 20 Ma, and the moderately extended domain from 31 Ma to 10 Ma. These ages may also be applicable to extensional deformation in this study area.

Summary

Rocks in the study area were affected by syn-volcanic structures, and Basin and Range extensional deformation. The syn-volcanic structures, related to the Vicks Peak and South Canyon Tuffs, are the oldest tectonic structures in the study area. Basin and Range extension developed in a late Oligocene least principle stress field oriented about N63E to N70E. Basin and Range fault patterns were

controlled by pre-Tertiary basement fractures in the southeast, an Oligocene sub-volcanic pluton in the north, and syn-volcanic faults in the central part of the study area. The Oligocene volcanic strata has undergone extension which increases from about 20% to almost 100% from south to north in the study area.

CHAPTER 5

CHEMISTRY

Introduction

Major element analyses of 3 ash-flow tuffs and 7 shallow intrusives, were done by the X-ray fluorescence method in order to chemically characterize the rocks in the study area. Analyses of the ash-flow tuffs are presented in Table 4, and of the intrusive rhyolites in Table 5. The coefficients of variation for each major element, calculated from 3 separate analyses of one ash-flow tuff sample (84-5-3), are presented in Table 4. Ion selective electrode analyses for fluorine and chlorine in the intrusive rocks are presented in Table 5.

All of the rocks analyzed (located on Plate 4) are rhyolites, and almost all of them contain $>75\%$ SiO_2 . The rhyolites average about 5% K_2O , placing this study area outside of a high- K_2O anomaly (characterized in rhyolites by K_2O contents as high as 10.4% , and Na_2O contents as low as 0.2%) that affects Oligocene to Miocene rocks throughout the Socorro area (D'andrea-Dinkelman and others, 1983).

Table 4. Major element chemical data of the South Canyon Tuff, Lemitar Tuff, and the tuff of The Park from this study area. Also shown are the coefficients of variation for each element (determined from 3 analyses of sample 84-5-3).

Sample	SiO ₂	TiO ₂	Al ₂ O ₃	Fe ₂ O ₃ *	MnO	MgO	CaO	Na ₂ O	K ₂ O	P ₂ O ₅	LOI	Total
84-4-7	77.45	0.14	12.27	0.86	0.04	0.02	0.40	3.41	5.00	0.02	0.46	100.07
84-4-6 [†]	78.20	0.12	11.93	0.82	0.04	0.01	0.35	3.35	4.86	0.02	0.37	100.71
84-4-5	77.54	0.12	12.00	0.78	0.04	0.07	0.37	3.34	4.85	0.02	0.61	99.74
84-4-4	77.61	0.10	12.13	0.70	0.04	0.09	0.35	3.87	4.66	0.02	0.70	99.82
84-4-3	76.74	0.10	12.41	0.60	0.04	0.11	0.38	3.77	4.81	0.02	0.82	99.78
84-4-2	76.78	0.09	12.77	0.69	0.06	0.16	0.35	3.52	4.86	0.02	1.10	100.41
84-5-5	72.33	0.35	14.52	1.84	0.05	0.17	0.30	2.52	6.98	0.03	1.07	100.14
84-5-4	73.60	0.27	14.08	1.42	0.02	0.11	0.55	3.58	5.54	0.04	0.64	99.85
84-5-3 [°]	75.67	0.18	12.98	1.09	0.05	0.08	0.36	3.44	5.58	0.02	0.51	99.51
C.O.V. (%)	0.4	3.4	0.6	2.8	5.5	2.5	0.8	2.5	0.7	8.7		
84-5-2	78.02	0.16	11.83	0.92	0.07	0.03	0.29	3.20	5.13	0.02	0.34	100.01
84-5-1	77.86	0.16	11.86	0.92	0.08	0.07	0.30	3.30	5.10	0.03	0.37	100.03

[†]average of two analyses

[°]average of three analyses

*total Fe

C.O.V.=coefficient of variation

Table 5. Major element chemical data of rhyolite intrusives in the study area.

Sample no.	SiO ₂	TiO ₂	Al ₂ O ₃	Fe ₂ O ₃ *	MnO	MgO	CaO	Na ₂ O	K ₂ O	P ₂ O ₅	F	Cl	LOI	Total
84-6	77.34	0.10	12.44	0.79	0.04	0.06	0.43	3.21	5.15	0.02	0.03	0.003	0.64	100.22
84-7	77.00	0.12	12.37	0.85	0.05	0.09	0.43	3.40	5.27	0.02	0.02	0.005	0.67	100.28
84-8	79.60	0.10	10.96	0.75	0.05	-	0.30	2.95	4.69	0.02	0.02	0.01	0.71	100.11
84-9†	77.02	0.11	12.51	0.79	0.07	0.01	0.29	3.52	5.07	0.02	0.03	0.002	0.51	99.88
84-10	77.20	0.11	12.39	0.81	0.06	0.02	0.39	3.53	4.84	0.02	0.03	0.003	0.57	99.94
84-11	77.38	0.11	12.61	0.79	0.04	-	0.27	3.37	4.93	0.02	0.03	0.003	0.43	99.95
84-12	77.15	0.12	12.57	0.83	0.06	0.03	0.32	3.31	5.06	0.02	0.03	0.002	0.65	100.11
84-13	77.74	0.12	12.30	0.88	0.07	0.03	0.29	3.55	4.95	0.02	0.06	0.002	0.41	100.36
84-27	77.01	0.18	12.43	0.97	0.05	-	0.17	3.61	4.79	0.004	na	na	0.46	99.61
84-159	70.94	0.38	14.19	1.93	0.05	0.28	0.41	3.16	7.42	0.06	na	na	0.41	99.37

† average of two analyses

* total Fe

na=no analysis

-not detected

Ash-flow tuffs

Samples from vertical sections of the tuff of The Park (84-5-1,2,3), the Lemitar Tuff (84-5-4,5), and the South Canyon Tuff (84-4-2,3,4,5,6,7) were analyzed for major elements (Table 4). The Tuff of The Park, and the South Canyon Tuff are both high silica rhyolites ($>75\%$ SiO_2), and show very little vertical variation. The South Canyon Tuff shows a slight upward increase in TiO_2 (0.09%-0.19%), and a significant upward decrease in MgO (0.16%-0.02%). The Lemitar Tuff is less silicic than the other tuffs (72-73% SiO_2). The upper sample of the Lemitar (84-5-5) appears to be altered, being enriched in K_2O (7.0%), and depleted in Na_2O (2.5%) and CaO (0.3%) compared to the lower sample (84-5-4) (K_2O , 5.5%; Na_2O , 3.6%; CaO , 0.5%).

Intrusives

All of the intrusive rocks analyzed in the study area are high- K_2O (5%), high- SiO_2 rhyolites ($>77\%$; Table 5). Of the first stage rhyolites, two samples of the rhyolite of Drift Fence Canyon (84-8,9), and one of the rhyolite of Exter Canyon (84-159), which is pervasively altered, were analyzed. Of the second stage rhyolites, two samples of the rhyolite of Cave Peak (84-12,13), and one each of the rhyolite of Horse Mountain (84-10), rhyolite of Wilson Hill (84-11), and rhyolite of little Black Mountain (84-27) were

analyzed. Two analyses of the rhyolite of Wildcat Peak (84-8,9), a third stage intrusive, were analyzed. Sample (84-8) is higher in SiO_2 (79.6%), and lower in Al_2O_3 (11.0%) than all the other rhyolites in the study area, and is probably altered.

CHAPTER 6
PALEOMAGNETISM

Introduction

Paleomagnetic data presented in this paper is part of a larger study being done by Bill McIntosh at the New Mexico Institute of Mining and Technology. More detailed descriptions of laboratory procedures and the quality of the data will be presented in his forthcoming Ph.D. dissertation. Preliminary results of his study are published in McIntosh, 1983.

Regional ash-flow tuffs (La Jencia, Vicks Peak, Lemitar, and South Canyon Tuffs) were analyzed for paleomagnetic polarity and anisotropy of susceptibility data. All of the sample sites are located on Plate 4. Two local ash-flow tuff units (tuff of The Park, and tuff of Rosedale Canyon) and two intrusive rhyolites (rhyolite of Drift Fence Canyon, and rhyolite of Cave Peaks) were also analyzed. Both of these intrusive rhyolites have reversed polarities.

Polarity

Polarity data for the ash-flow tuffs is presented in Figures 34,35 along with the average paleopole positions for each regional unit outside this study area. All of the ash-flow tuffs in the study area are reverse polarized, except for the Lemitar Tuff.

Anisotropy of susceptibility

Magnetic anisotropy of susceptibility is a measurement of the orientation of elongated magnetic mineral grains. Anisotropy of susceptibility data is plotted as azimuths with cones of confidence (95% level) along with field measurements of aligned pumice fragments in Figures 5,7,9, and 28. The cones of confidence are narrowest for samples that are in lineated tuff, and the azimuths agree remarkably well with nearby field measurements of lineated pumice.

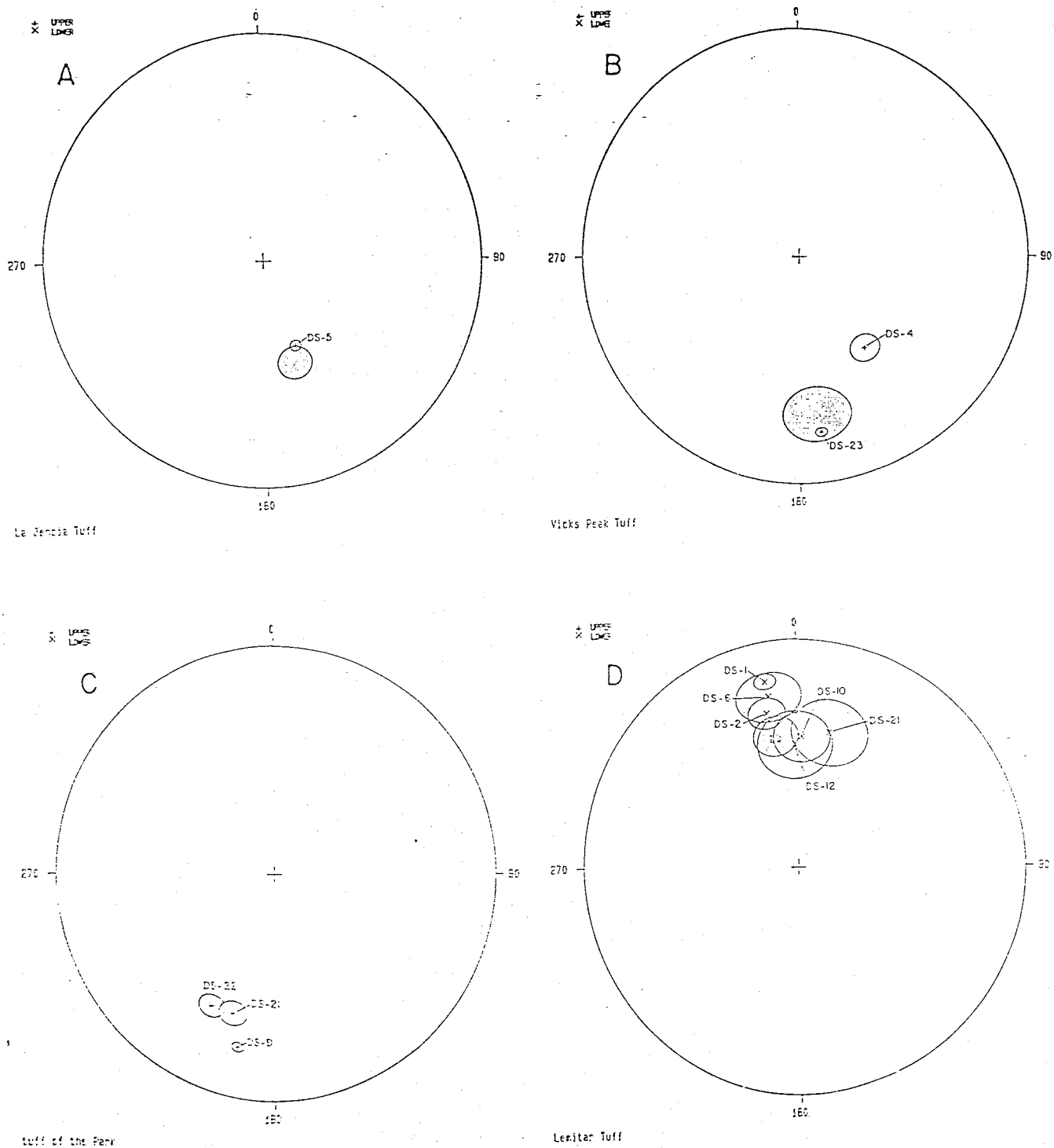


Figure 34. Paleomagnetic pole positions for samples of the La Jencia Tuff (A), Vicks Peak Tuff (B), tuff of The Park (C), and the Lemitar Tuff (D) from this study area. Average pole positions for samples outside this study area are shown with stippled patterns.

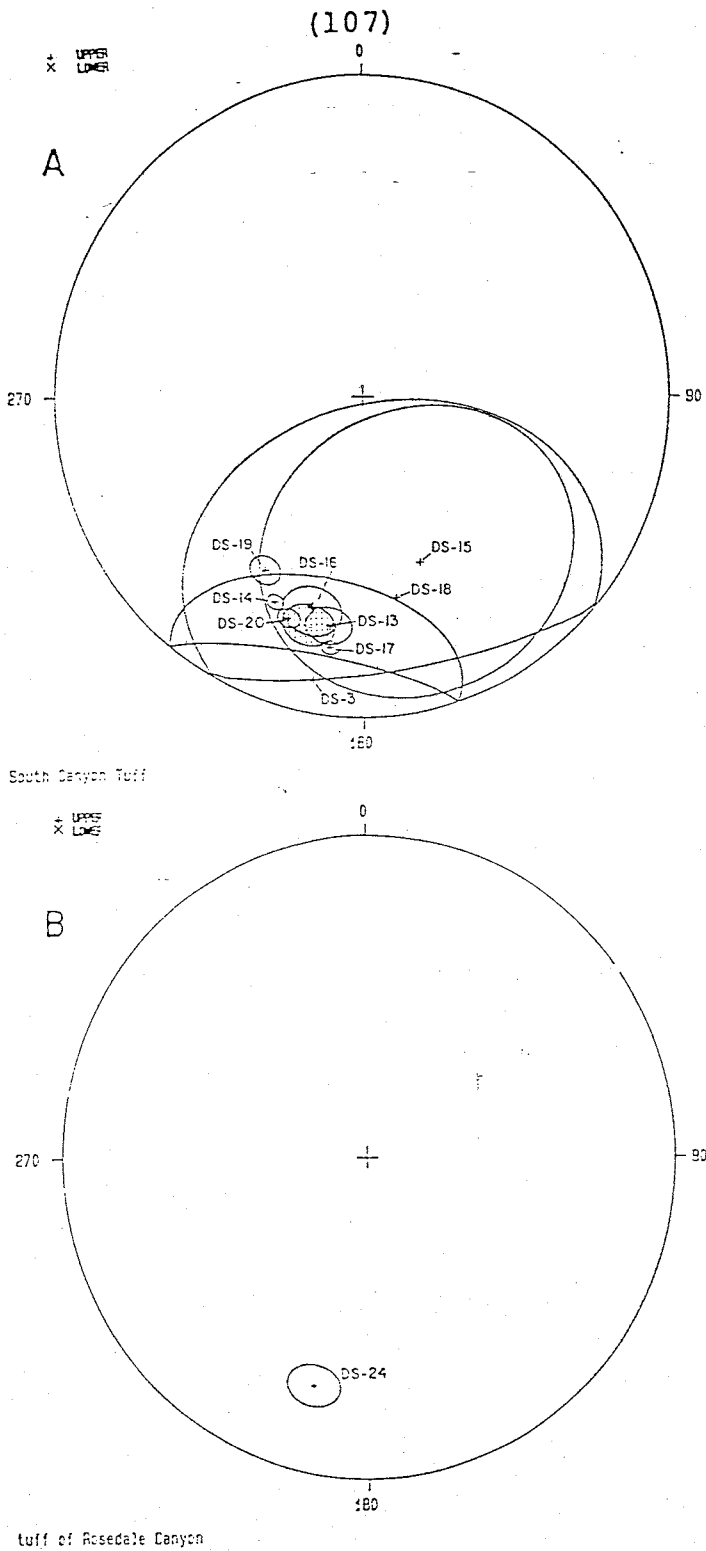


Figure 35. Paleomagnetic pole positions for samples of the South Canyon Tuff (A), and the tuff of Rosedale Canyon (B) from this study area. The average pole position for samples of the South Canyon Tuff from outside this study area is shown with a stippled pattern in (A).

CHAPTER 7
CONCLUSIONS

Conclusions

The major conclusions from this work are listed here.

(1) In the southeast part of the study area, the Vicks Peak Tuff is downfaulted and buried by local volcanic units. Subsidence in this area is thought to be related to collapse of the Vicks Peak Tuff's cauldron somewhere in the southern San Mateo Mountains. (2) The southeast part of the study area was uplifted and eroded before deposition of the Lemitar Tuff. This uplift may be related to resurgence of the Vicks Peak Tuff's cauldron. (3) The Lemitar Tuff and older rocks in the study area are truncated to the west by a structural basin related to eruption of the South Canyon Tuff. The north end of this basin is the southern extension of the South Canyon Tuff's cauldron. (4) A vent for the South Canyon Tuff is located along its southeast cauldron margin. (5) The wind was blowing from the southwest in late Oligocene time. (6) Late Oligocene volcanic rocks, erupted from vents in this study area, are all high-K₂O (5%), high SiO₂ rhyolites. (7) Most of the rocks in this study area were not affected by the K₂O metasomatic enrichment event that altered Oligocene to Miocene rocks throughout the

Socorro area. (8) Rocks in the study area were deformed by late Oligocene to Miocene Basin and Range extensional stresses oriented about N63E. Extension, which tilted blocks to the east from 5-50 degrees, increases from about 20% in the south to about 100% in the north.

POSTSCRIPT

During the completion of this thesis, new information was acquired which strongly supports alternative correlations for 4 stratigraphic units in this study (tuff of the Park, unit of East Red Canyon, part of the South Canyon Tuff, and some of the second stage rhyolites). This information and the suggested revisions were acquired too late to be included here, but are summarized below. The changes are being incorporated into this text which will then be published as a New Mexico Bureau of Mines and Mineral Resources Open-file Report. The interested reader is urged to seek this report.

Paleomagnetic pole positions for ash-flow tuff units provide the basic data for the alternative interpretations. Pole positions from the tuff of The Park are similar to the average South Canyon Tuff pole position. Pole positions of what was mapped as the South Canyon Tuff, overlying the sedimentary unit of East Red Canyon in the south half of the area, are coincident with pole positions of a tuff which overlies the South Canyon Tuff about 10km to the northwest (Donze, 1980; McIntosh, personal communication).

Reexamination of tuff of The Park outcrops in section 23, T6S, R6W shows that most of them are actually lower Lemitar Tuff. Tuff of The Park exposures in the southwest corner of

The Park, and in the Allen Spring area (Plate 1) are paleomagnetically reversely polarized, and are interpreted to be the upper South Canyon Tuff.

Major implications of these alternative interpretations are: 1) the tuff of The Park does not exist; 2) the unit of East Red Canyon is younger than the South Canyon Tuff and correlative with the unit of North Canyon; 3) the tuff overlying the unit of East Red Canyon is a younger unit correlative with Donze's (1980) uppermost ash-flow tuff; and 4) some of the second stage rhyolites (Cave Peaks and Horse Mountain Canyon lavas) can be younger than the South Canyon Tuff.

REFERENCES

- Atwood, G. W., 1982, Geology and geochemistry of the San Juan Peak area, San Mateo Mountains, New Mexico: with special reference to the geochemistry, mineralogy, and petrogenesis of an occurrence of riebeckite-bearing rhyolite: M. S. thesis, University of New Mexico, 156 pp.
- Bobrow, D. J., 1984, Geochemistry and petrology of Miocene silicic lavas in the Socorro-Magdalena area of New Mexico: M. S. thesis, New Mexico Institute of Mining and Technology, 145 pp.
- Brookfield, M. E., 1977, The origin of bounding surfaces in ancient aeolian sandstones: *Sedimentology*, v. 24, p. 303-332.
- Brown, D. M., 1972, Geology of the southern Bear Mountains, Socorro County, New Mexico: M. S. thesis, New Mexico Institute of Mining and Technology, 110 pp.; New Mexico Bureau of Mines and Mineral Resources, Open-file Report 42, 110 pp.
- Chamberlin, R. M., and Osburn, G. R., 1984, Character and evolution of extensional domains in the Socorro area of the Rio Grande Rift, central New Mexico (abs): *Geologic Society of America, Abstracts with programs*, v. 16, no. 6, p. 467.
- Chapin, C. E., 1979, Evolution of the Rio Grande Rift - a summary: in Riecker, R. E., *Rio Grande Rift: tectonics and magmatism*: American Geophysical Union, p. 1-5.
- Deal, E. G., 1973, Geology of the northern part of the San Mateo Mountains, Socorro County, New Mexico - a study of a rhyolite ash-flow tuff cauldron and the role of laminar flow in ash-flow tuffs: Ph. D. dissertation, University of New Mexico, 136 pp.
- Deal, E. G., and Rhodes, R. C., 1976, Volcano-tectonic structures in the San Mateo Mountains, Socorro County, New Mexico: in Elston, W. E., and Northrop, S. A. (eds.), *Cenozoic volcanism in southwestern New Mexico*: New Mexico Geological Society, special publication 5, p. 51-56.
- Deer, W. A., Howie, R. A., and Zussman, J., 1966, *An introduction to the rock forming minerals*: Longman, 528 pp.

- D'andrea-Dinkelman, J. F., Lindely, J. I., Chapin, C. E., and Osburn, G. R., 1983, The Socorro K₂O anomaly: A fossil geothermal system in the Rio Grande Rift: in Chapin, C. E., and Callender, J. F., (eds.), New Mexico Geologic Society, Guidebook to 34th field conference, p. 76-77.
- Donze, M. A., 1980, Geology of the Squaw Peak area, Magdalena Mountains, Socorro County, New Mexico: M. S. thesis, New Mexico Institute of Mining and Technology, 120 pp., New Mexico Bureau of Mines and Mineral Resources, Open-file Report 123, 131 pp.
- Fink, J. H., 1984, Spatial variations in the volume, texture, and structure of silicic domes fed by dikes (abs): Geologic Society of America, Abstracts with programs, v. 16, no. 6, p. 509.
- Furlow, J. W., 1965, Geology of the San Mateo Peak area, Socorro County, New Mexico: M. S. thesis, University of New Mexico, 83 pp.
- Hunter, R. E., 1977, Basic types of stratification in small eolian dunes: Sedimentology, v. 24, p. 361-387.
- Jahns, R. H., 1944, Beryllium and tungsten deposits of the Iron Mountain District, Sierra and Socorro Counties, New Mexico: U. S. Geologic Survey Bulletin 945-C, 79 pp.
- Kedzie, L. L., Sutter, J. F., and Chapin, C. E., 1985, High-precision ⁴⁰Ar/³⁹Ar ages of widespread Oligocene ash-flow tuff sheets near Socorro, New Mexico (abs): Geologic Survey of America, Abstracts with programs, in press.
- Lambert, P. W., 1968, Quaternary stratigraphy of the Albuquerque area, New Mexico: Ph.D. dissertation, University of New Mexico, 329 pp.
- McIntosh, W. C., 1983, Preliminary results from a paleo- and rock magnetic study of Oligocene ash-flow tuffs in Socorro County, New Mexico: in Chapin, C. E., and Callender, J. F. (eds.), New Mexico Geologic Society, Guidebook to 34th field conference, p. 205-210.
- Neubert, J. T., 1983, Mineral investigations in the Apache Kid and Withington wilderness areas, Socorro County, New Mexico: U. S. Bureau of Mines open file report MLA 72-83, 35 pp.

- Osburn, G. R., 1978, Geology of the eastern Magdalena Mountains, Water Canyon to Pound Ranch, Socorro County, New Mexico: M. S. thesis, New Mexico Institute of Mining and Technology, 150 pp.; New Mexico Bureau of Mines and Mineral Resources Open-file report 113, 160 pp.
- Osburn, G. R., 1982, Gallery of Geology: New Mexico Geology, v. 4, no. 3, p. 38.
- Osburn, G. R., and Chapin, C. E., 1983, Nomenclature for Cenozoic rocks of northeast Mogollon-Datil volcanic field, New Mexico: New Mexico Bureau of Mines and Mineral Resources, Stratigraphic Chart 1, 7 pp., 2 sheets.
- Shultz, A. W., 1984, Subaerial debris-flow deposition in the upper Paleozoic Cutler Formation, western Colorado: Journal of Sedimentary Petrology, v. 54, p. 759-772.
- Sparks, R. S. J., 1976, Grain size variations in ignimbrites and implications for the transport of pyroclastic flows: Sedimentology, v. 23, p. 147-188.
- Tonking, W. H., 1957, Geology of Puertecito quadrangle, Socorro County, New Mexico: New Mexico Bureau of Mines and Mineral Resources, Bulletin 41, 67 pp.
- Wright, J. V., and Walker, G. P., 1977, The ignimbrite source problem: Significance of a co-ignimbrite lag-fall deposit: Geology, v. 5, p. 729-73 .
- Zoback, M. L., Anderson, R. E., and Thompson, G. A., 1981, Cainozoic evolution of the state of stress and style of tectonism of the Basin and Range Province of the western United States: Philosophical Transactions of the Royal Society of London, v. 300, p. 407-434.

APPENDIX A

PETROGRAPHIC PROCEDURES

Observations of 50 standard thin sections of ash-flow tuffs (43), rhyolite intrusives and lavas (4), and sandstones (3) are presented in this paper. Thin sections were studied on Nikon type 102 and type 104 binocular petrographic microscopes. The Geologic Society of America rock color chart was used to standardize color names.

So that sanidine could be easily distinguished from quartz, volcanic thin sections were stained with sodium cobaltinitrate, following procedures described by Deer and others (1966, p. 311). Crystal-poor one feldspar tuffs required longer etching times (60-90 seconds) than the quartz-feldspar bearing tuffs (20-40 seconds). Phenocryst abundances of volcanic rocks were visually estimated from thin sections, and pumice and lithic abundances from hand specimens. Three sandstone thin sections were point counted on a Swift automatic point counter.

APPENDIX B

GEOCHEMICAL PROCEDURES

Twenty samples of silicic ash-flow tuffs (11), and lavas (9) were analyzed for major elements by x-ray fluorescence on a Rigaku 3064 spectrometer at New Mexico Bureau of Mines and Mineral Resources. Rocks were selected by checking the feldspars and biotite for obvious signs of alteration; all samples with >5% lithics were rejected. Samples were trimmed of weathered material in the field to make specimens weighing at least 1kg. These were later reduced to pieces <4cm using a hammer and a steel plate. A steel jaw crusher and steel rolls were then used to reduce the sample to pieces <5mm. A portion of each sample was then ground in a Tema mill to produce an approximate 200-mesh powder.

Procedures used for preparation of the powdered samples for major element analysis are described by Bobrow (1984, p. 137). One sample (S-37) was analyzed for iron and trace elements by instrumental neutron activation. Procedures for this sample are described by Bobrow (1984, p. 138).

Chlorine and fluorine analyses were done at the New Mexico Bureau of Mines and Mineral Resources by ion selective electrode.

APPENDIX C

PALEOMAGNETIC PROCEDURES

Twenty four outcrops of ash-flow tuff and intrusive rhyolite were sampled for paleomagnetism in the study area (Plate 4). Structural attitudes of eutaxitic foliation in ash-flow tuff samples were measured with a magnetic compass at each outcrop site. Regional attitudes were used for structural correction of intrusive rhyolite samples (DS-7,8), and for two flow-banded and contorted ash-flow tuff samples (DS-11,23). Eight 2.5cm diameter cores, 5 to 10cm in length, were drilled from each outcrop site using a gasoline-powered, water-cooled, diamond-bit drill produced by Roc Drill Systems. Cores were oriented with magnetic compass and suncompass and later sliced into 2.2cm lengths.

Paleomagnetic measurements were performed on a Schonstedt SSM-1 spinner magnetometer interfaced with a Northstar microcomputer. After initial measurements of natural remanent magnetization, samples were subjected to stepwise alternating field demagnetization in peak fields of up to 40 milliteslas using a non-commercial single-axis alternating field demagnetization device. The remanence directions of samples were remeasured after each demagnetization step and average directions and statistics were calculated for the eight samples from each site. Data

(118)

from the demagnetization step which produced the smallest within-site dispersion was used to characterize the remanence direction at each site. The anisotropy of susceptibility of the ash-flow tuff samples was determined using a Sapphire Instruments SI-2 susceptibility bridge interfaced with an Apple II computer.